06.30.2025

BERKELEY JOURNAL OF



Entomology and Agronomy Studies (BJEAS) Vol. 8 No. 1

D SUBSURFACE MODELING OF LEACHATE INFILTRATION AND DISTRIBUTION IN A TYPICAL CASSAVA PROCESSING SITE USING INTEGRATED GEOPHYSICAL AND GEOCHEMICAL TECHNIQUES IN APETE, SOUTH-WEST NIGERIA

¹ISHOLA S. A., ².KUGBERE, E., ¹.MOSURO, G.O., ³BIERE, P. E., ¹.OGUNGBADE, O., ¹. OLOYEDE, E.A.

¹Department of Earth Sciences, Olabisi Onabanjo University Ago-Iwoye, P.M.B 2002, Ago-Iwoye, Ogun State, Nigeria. ²Department of Physics, Southern Delta University, Ozoro, Ozoro Delta State Nigeria. ³Department of Physics, Niger Delta Wilberforce Island, Bayelsa State, Nigeria

different

Corresponding Author: ishola.sakirudeen@oouagoiwoye.edu.ng

DOI Link: https://doi.org/10.70382/bjeas.v8i1.011

significant concentration of

assava mill effluent (CME) contains a

ABSTRACT

■ hazardous inorganic components, especially cyanide (CN) and cyanogenic glucosides which can result in environmental problems. This study seeks to evaluate the impacts of CME on groundwater and the level of leachate infiltration into the subsurfa ce in a cassava processing site using integrated geophysical and geochemical techniques in Apete. 3-D Electrical Resistivity Imaging (ERI), Vertical Electrical Sounding (VES) and geochemical evaluations alongside well inventories were used to characterize and delineate the subsurface lithology to determine the extent of leachate infiltrations in the study area. A 2D electrical resistivity survey was performed along five (5) profile lines, each 70m long and spaced 5m apart, using the Wenner configuration with varying electrode spacings. This survey was complemented by a 1D electrical survey to produce a 3D output and three (3) Vertical

Introduction

The term "waste" encompasses materials that are surplus to the primary product and are discarded by the initial user. This surplus can be a byproduct of raw material extraction and processing, consumption of end products, and various other human activities. According to NISP (2003), waste can also refer to any inevitable materials generated during an activity that lacks immediate economic demand and requires disposal. Waste is commonly categorized as solid, liquid, or gaseous, with a specific focus on liquid waste herein. Liquid waste can percolate into the subsoil, leading to soil and groundwater or aquifer contamination if the subsoil's leachate migration protective capacity is insufficient.

BERKELEY RESEARCH & PUBLICATIONS INTERNATIONAL

Bayero University, Kano, PMB 3011, Kano State, Nigeria. +234 (0) 802 881 6063, berkeleypublications.com



Vol. 8, No. 1

Berkeley Journal of Entomology and Agronomy Studies

Electrical Soundings (VES) at locations where cassava effluents accumulated. The measured resistivity values were multiplied by the geometric factors to calculate apparent resistivity, which was then processed through ZONDRes3D resistivity and IP inversion software to create inverted 3D resistivity models. The resulting models were analyzed using X. Y. and Z. directional slice cuts. The 3-D resistivity images of the array were meticulously analyzed in terms of depth slices, resistivity inclines, and crosslines. The depth slices revealed leachate infiltration extending up to 40m, characterized by a resistivity ranging from (6-63 Ω m Ω m) across the x-direction, displaying a diminishing trend with profile depth where points of low resistivity value (≤10 Ωm) were identified as highly contaminated with CME. Varied levels of infiltration were observed at different distances. The results of three (3) VES revealed low resistivity values ranging from 13.0 to 65.5 Ω m in APETEVES1, 18 to 104.6 Ω m in VES 2 while the control VES displayed resistivity values of 103.8 to 340.9 Ωm in all the identified four layers. The results of the water level measurement and geochemical evaluations revealed depths of 1.77m to 4.60m which were inferred to be very shallow while Mn, Cd and Pb in the groundwater samples were found to be above the limits of set standard and occurrences were b attributable to the infiltration of CMEs into the subsurface groundwater system. The study found varying resistivity values in the soil, indicating leachate contamination that diminishes with depth. The low resistivities and shallow wells highlighted the extent of the groundwater system's vulnerability to contamination from cassava effluents.

Keywords: 3D modelling; CME; Geoelectric method; Apete; Cyanide; ZONDRes3D; Effluents

ver time, this phenomenon has evolved into an environmental concern (Ogundana et al., 2018; Ogbonna et al., 2008). The formation of leachate is a crucial component of municipal waste and is a consequence of water infiltration through landfills or other activities such as cassava processing, which may result in the release of liquid waste through precipitation or surface run-off. This process can enhance biochemical reactions, leading to an inherent rise in water content within the waste (Giang et al., 2018). A profound factor out of numerous ones influencing the rate at which waste is generated is biological population increase (Parlinggoman, 2011; Qadri et al., 2020). Varying attributes of wastes are governed by their compositions, the amount of wastes present as well as the rainfall intensity (Purwanta et al., 2007). Thus, leachate has the potential to cause environmental pollution, especially soil, groundwater, and surface water pollution, if it is not appropriately managed (Ulfani et al., 2019; Lavrova and Koumanova, 2010; Yatim and Mukhlis, 2013; Riogilang, 2021; Azizah, 2016; Pratiwi et al., 2018; Yadi, 2017; Tampubolin et al., 2020) and if wastes are not well managed, it will inadvertently cause environmental pollution and clinical conditions because leachates are toxic (Fitrianti, 2018; Karami, 2022; Pratama et al., 2020; Nubatonis et al., 2021). Cassava processing necessitates the conversion of lethal cyanogenic glucosides and cyanides, which manifest as cassava mill effluents (CMEs) and pose environmental hazards (Padmaja, 1995). During cassava harvesting and processing,





Vol. 8, No. 1

Berkeley Journal of Entomology and Agronomy Studies

plant-borne hydrolases cause the conversion of cyanogenic glucosides and cyanides into byproducts that are subsequently released into the soil. Additionally, microbial contamination and the resultant generation of wastewater during the processing of such produce can lead to the formation of rotten produce. (Siller and Winter, 1998; Ogilvy et al., 2002; Okechi et al., 2012). Obueh and Odesiri (2016) observed that the frequent disposal of CMEs into the soil alters the microbiological, mineral, and physicochemical compositions of the soil environment surrounding the mills. Furthermore, depending on the hydraulic conductivity of the geological material, CMEs may migrate to other locations. According to Nwakauda et al., (2012), Igbinosa and Igiehon (2015), and Igbinosa (2015), heavy metals such as Fe, Zn, Mn, Al, Pb, and Cu are significantly more prevalent in soils in proximity to cassava mills. Osakwe (2012) also remarked that CME lowers soil pH and results in elevated levels of available phosphorus, total organic carbon, total nitrogen, electrical conductivity, and cation exchange capacity in the soils. Leachate derived from CMEs may contain inorganic chemical constituents similar to those found in landfill leachate. If not adequately treated to eliminate hazardous components before disposal, leachate can infiltrate and migrate to groundwater or surface water, posing health risks to human populations (Ganiyu et al., 2018). This necessitates the involvement of environmental geophysicists in investigating leachate migration (Ganiyu et al., 2018; Onwhugbere-Asuma et al., 2014).

Assessing the extent of groundwater contamination has assumed increasing significance due to the human right to access clean water and the essential requirement for economic development. Despite these imperatives, inadequate waste disposal practices have heedlessly led to environmental pollution, often close to uncontrolled waste sites located near boreholes and wells, which serve as sources of drinking water for local communities (Kirsch, 2006; Nasir et al., 2010; Awoibi and Ademakinwa, 2018). The investigation of leachate plume migration often utilizes geotechnical and geophysical methods. Geotechnical methods involve the collection of in-situ soil samples at the dump site, while geophysical methods entail measuring variations in the earth's physical properties (Loke, 1999). Among geophysical exploration methods, the electrical method has gained prominence as it offers superior visualization of the subsurface plume by measuring the electrical conductivity of the leachate and subsurface variations (Loke, 1999; Meju, 2000; Porsani et al., 2004; Dahlin et al., 2006; Oyedele, 2009; Cristina et al., 2012; Sechman et al., 2013). Importantly, this method causes no physical harm to the environment and is cost-effective. 2-D direct current (DC) electrical survey methods have been effectively utilized over the years in measuring the apparent resistivity of subsurface layers at dumpsites. Loke (2004) emphasized that variables such as the presence of fluid in the subsurface, porosity, and the chemical and ionic composition of subsurface materials can impact the apparent resistivity value. However, recent interest has shifted towards 3-D electrical resistivity surveying to map subsurface electrically conductive contamination plumes in the unsaturated zone and electrically conductive lithological units such as clay. 3-D electrical resistivity surveying offers Modeling the leachate distribution beneath the soil surface can be achieved through the application of



Vol. 8, No. 1

Berkeley Journal of Entomology and Agronomy Studies

geoelectric techniques (Nilasari et al., 2011; Sedana et al., 2015; Alao, 2022). Geoelectric techniques are non-invasive geophysical field applications for determining resistivity changes of subsurface rock by the passage of high-voltage DC electricity into the subsurface (Broto and Afifah. 2008). The observed differentiation of rock's resistivity can be utilized in identifying the leachate distribution in the subsurface (Putra et al., 2012). The adopted geoelectric technique of geophysical investigation utilized in this study was the Wenner array where systems of constant electrode spacing standards are administered (Priambodo et al., 2011). The significance and merits of Wenner array is that the reading accuracy of the voltage at the potential electrode is better with relatively large numbers since the proximity of the potential electrode to the current electrode reasonably close and it is more detailed in describing the lateral direction (Meilasari et al., 2023). The Wenner array has been successfully applied to delineate subsurface leachate distribution both in 2D and 3D (Pratama et al., 2020; Ojo et al., 2022; Daruwati, 2019; Feng et al., 2020; Mosuro et al., 2019). Loke (2004) emphasized that variables such as the presence of fluid in the subsurface, porosity, and the chemical and ionic composition of subsurface materials can impact the apparent resistivity value. However, recent interest has shifted towards 3-D electrical resistivity surveying to map subsurface electrically conductive contamination plumes in the unsaturated zone and electrically conductive lithological units such as clay. 3-D electrical resistivity surveying offers enhanced visualization compared to 2-D DC electrical resistivity methods. Therefore, this research aims to delineate the leachate infiltration pattern into the subsurface layer and intends to investigate the impact of CMEs on the subsoil and the groundwater using geophysical and hydrogeochemical groundwater modeling at the Apete cassava processing site, South-West, Nigeria.

Study Area

Location and Accessibility

The research site is located in a suburb of Apete Township in Oyo State, Nigeria. It is positioned approximately 0.73 kilometers west of Apete Motor Garage and about 1.7 kilometers south of Polytechnic Ibadan. The area is restricted by Latitude 7°27'02" and 7°27'03" North of the equator and longitude 3°52'13" and 3°52'11" East of the Greenwich Meridian. Major roads and footpaths facilitate access to this area. Figure 1 is a field photograph showing the cassava processing activities in the study area; Figure 2 is a Satellite map of the study area showing the surveyed area and profile lines and Figure 3 is the Data acquisition map of the study area.

Climate and Vegetation

The climate of the study area is characterized by a tropical wet and dry climate with a lengthy wet season and relatively constant temperatures throughout the year. The wet season runs





Vol. 8, No. 1

Berkeley Journal of Entomology and Agronomy Studies

from March through October, though August sees somewhat of a lull in precipitation. This lull divides the wet season into two different wet seasons. November to February forms the area's dry season, during which the typical West African harmattan occurs. The mean total rainfall of the area is approximately 1,230 millimeters or 48 inches, falling over about 123 days. There are two peaks for rainfall, June and September (Egbinola and Amanambu 2014). The mean daily temperature is 26.46 °C or 79.63 °F, the mean minimum is 21.42 °C or 70.56 °F, and the relative humidity is 74.55% (Amanambu (2015). The area is naturally drained by four rivers with many tributaries: the Ona River in the North and West; the Ogbere River towards the East; the Ogunpa River flowing through the area and the Kudeti River in the Central part of the metropolis. Ogunpa River is a third-order stream with a channel length of 12.76 km and a catchment area of $54.92 \, \mathrm{km^2}$. Lake Eleyele is located in the northwestern part of the area, while the Osun River and the Asejire Lake border the area to the east. The vegetation pattern of the study area is a patchwork of broken forest, savannah woodland, dense thickets, and large tracts of forbs vegetation dominated by Chromolaena (Eupatorium) and Odorata (Siam weed) (Odjugo, 2010).

Berkeley Journal of Entomology and Agronomy Studies



Figure 1: A Field photograph showing the Study Area (Cassava processing site)

Berkeley Journal of Entomology and Agronomy Studies

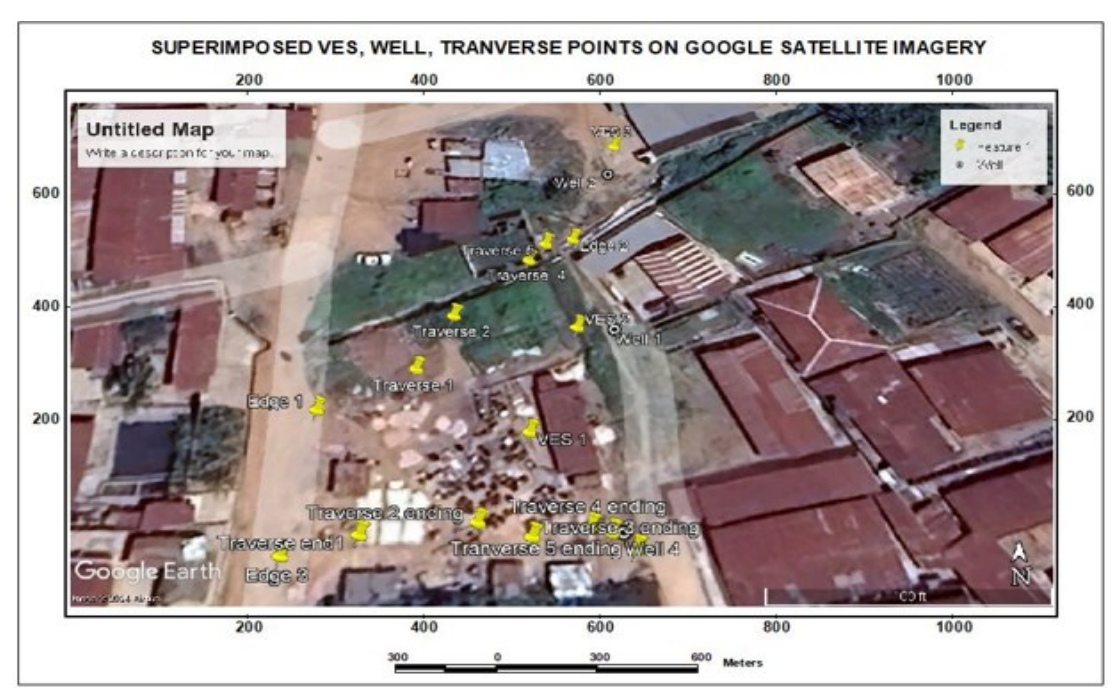


Figure 2: Satellite Map of the Study Area showing the survey area and profile lines.

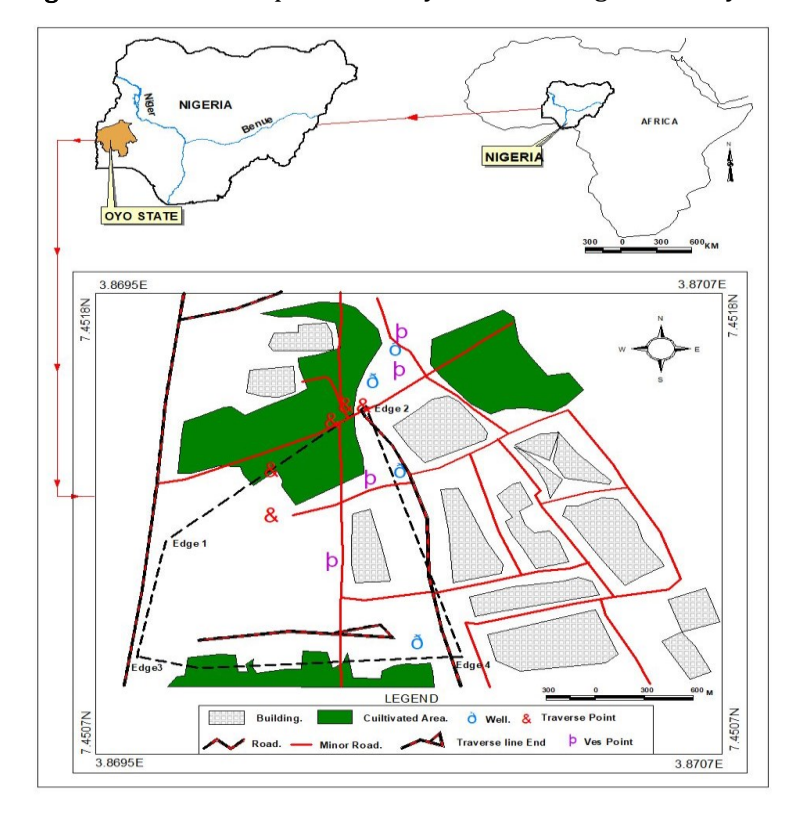


Figure 3: Data acquisition map of the Study Area

Geology of the Study Area

The study area underlain by three lithological units of the crystalline basement complex, comprising of migmatite-gneiss complex (quartzite, gneissic rocks); Low to medium grade metasediments (green schists facies, namely quartz schist and mica schist) and the pan African granitoids (older granites) which are syn

BERKELEY RESEARCH & PUBLICATIONS INTERNATIONAL

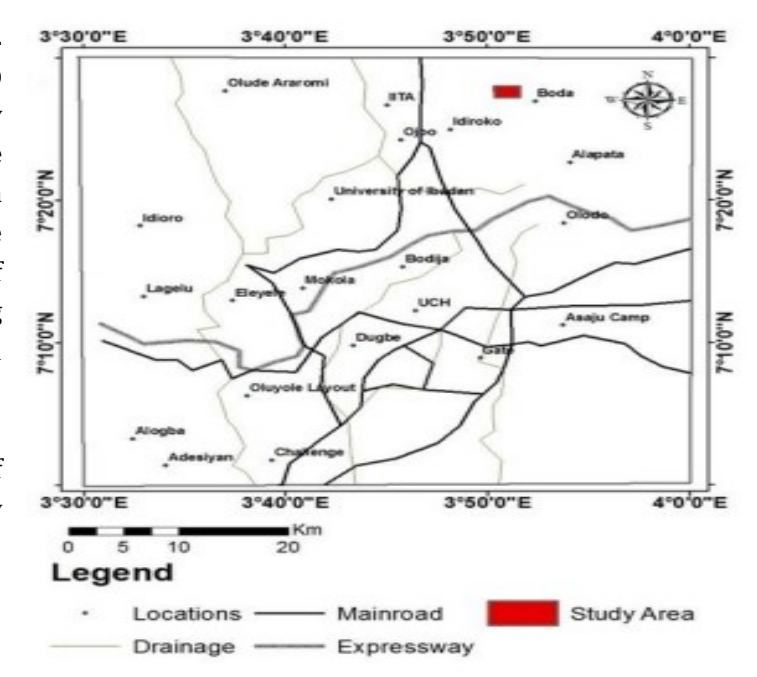
Bayero University, Kano, PMB 3011, Kano State, Nigeria. +234 (0) 802 881 6063, berkeleypublications.com



Berkeley Journal of Entomology and Agronomy Studies

to late tectonic intrusions. Figure 4 is the location map of Ibadan showing the Study Area amidst the neighbouring town in Ibadan (Adebo *et al.*, 2023) while Figure 5 is the geology map of the study area showing assemblages of rock types in the study area.

Figure 4: Location map of Ibadan indicating the Study Area (Adebo *et al.*, 2023)



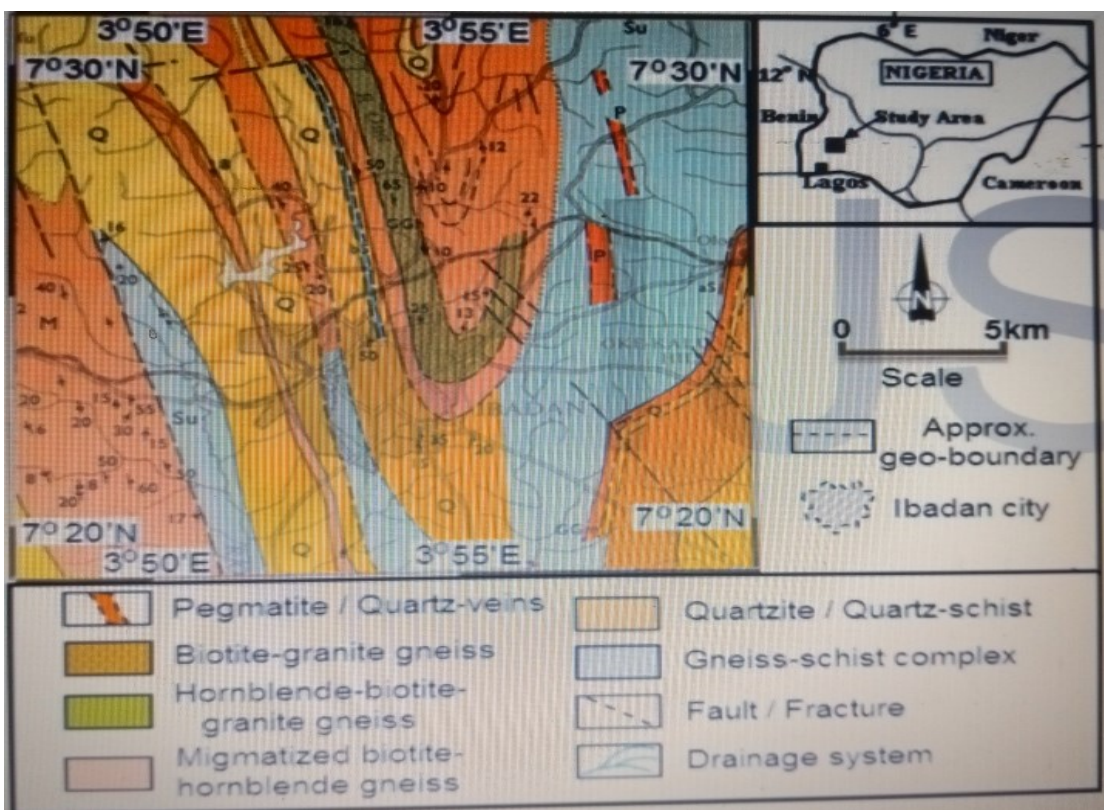


Figure 5: Geology map of the study area (Akinbiyi et al., 2018)



Vol. 8, No. 1

Berkeley Journal of Entomology and Agronomy Studies

Materials and Methods

Mechanisms of Electrical Resistivity Techniques and Solute Transportation

Electrical methods of geophysical investigations are centered on resistivity (or its inverse otherwise known as conductivity) contrasts of subsurface constituents. The electrical resistance, R of any given substance is akin to its physical dimension, cross-sectional area, A and length, L via the resistivity, ρ or its inverse, conductivity, σ by

$$\rho = \frac{1}{\sigma} = \frac{RA}{L} \qquad$$

Low frequency alternating current is utilized as source signals in the direct current resistivity surveys for evaluating subsurface resistivity distributions. Thus, the magnetic properties of the materials can be ignored (Telford et al., 1990) so that the reduction of electromagnetic equations of Maxwell can be attained as

where \bar{E} is the electric field in V/m, ζ is the charge density in C/ m^3 and ε_0 is the permittivity of free space ($\varepsilon_0 \cong 8.854 \times 10^{-12} \text{F/m}$). These aforementioned equations though applicable to the flow of direct current that are continuous; they can be equally utilized for the representation of the effects of alternating currents exhibiting low frequencies such that displacement current as well as induction effects can be ignored.

A complete homogeneous and isotropic earth medium of uniform resistivity is usually assumed. For a current in a continuous state flowing in an isotropic and homogeneous medium, the current density $\overline{\mathbf{d}}$ is connected to the electric field, \overline{E} through Ohm's law:

$$\overline{\mathbf{d}}_{e} = \sigma \overline{E}$$
4

The electric field vector \bar{E} can be illustrated as the gradient of the electric scalar potential.

$$\bar{E} = - \nabla \Phi$$
5

the combination of equation 2 and 5 resulted to the basic poisson's equation for electrostatic fields illustrated mathematically as

Vol. 8, No. 1

Berkeley Journal of Entomology and Agronomy Studies

$$\nabla^2 \Phi (p, q, r) = -\frac{1}{\varepsilon_0} \zeta(p, q, r)$$
6

The equation of continuity for a point in 3D spacing and timing t expressed by Dirac delta function is given as

$$\nabla \cdot \overline{\mathbf{d}}_{s}(\mathbf{p}, \mathbf{q}, \mathbf{r}, \mathbf{t}) = -\frac{\partial}{\partial t} \zeta(\mathbf{p}, \mathbf{q}, \mathbf{r}, \mathbf{t}) \delta(p) \delta(q) \delta(r)$$
.....7

In a typical electrical resistivity survey, the current sources are usually point sources. Therefore, the current and current density over a volume element, ΔV around a current source, I located at (p_s, q_s, r_s) are given by the work of Dey and Morrison, 1979 expressed as

$$\nabla \cdot \vec{\mathsf{d}}_{s} = \left(\frac{1}{\Delta \mathsf{V}}\right) \, \delta \, \left(p - p_{s}\right) \, \delta \, \left(q - q_{s}\right) \, \delta \, \left(r - r_{s}\right) \, \dots \, 8$$

Where δ represents the Dirac delta function. Thus, the potential distribution in the ground due to a point current source is given as

$$-\nabla \left[\sigma(p,q,r)\nabla \Phi(p,q,r)\right] = \left(\frac{1}{\Delta V}\right) \delta \left(p - p_{s}\right) \delta \left(q - q_{s}\right) \delta \left(r - r_{s}\right) \dots 9$$

The self adjoint partial differential equation that is strongly connected and non-separable elliptic equation of second order resulting in the subsurface potential distribution of an isotropic non-uniform 3D medium as a result of a point current source. Numerous techniques have been developed to determine the potential distribution that would be observed over a given subsurface structure. The potential, $\Phi(p,q,r)$ and the normal component of the current density, $\sigma\left(\frac{\partial\Phi}{\partial N}\right)$ are continuous across the boundary between two (2) media of different resistivities but the current lines are being refracted due to the resultant implications stipulated in the boundary conditions.

While considering the state of potential distribution due to point sources in a homogeneous half-space; all resistivity techniques employ an artificial source of current meant to be injected into the subsurface through point electrodes and the potential difference is consequently measured at other electrodes that are positioned in nearness to the flow of current. For a semi-infinite conducting layer of uniform resistivity (a completely homogeneous and isotropic medium) bounded by the ground surface as displayed in figure 6.

Berkeley Journal of Entomology and Agronomy Studies

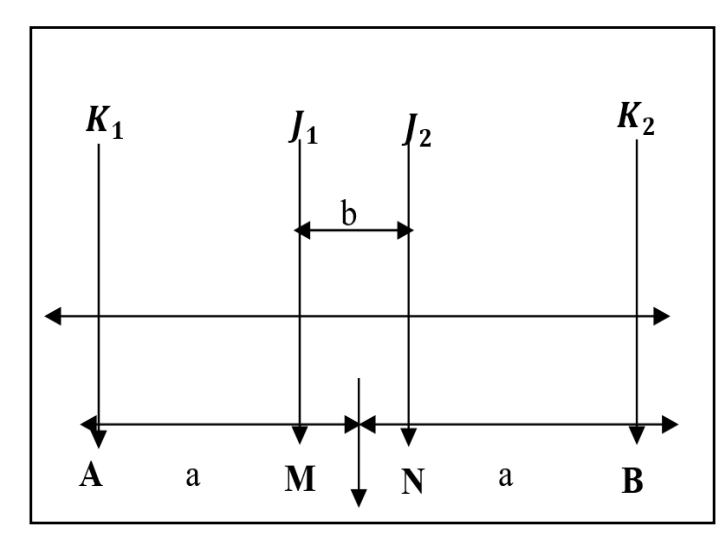


Figure 6: Configuration on the Field (Ishola, 2019)

A current of +1 is injected at a point K_1 into the subsurface. This current flows radially away from the point of injection, entering through the surface to the subsurface with its distribution being uniform over a hemispherical shell in a subsurface zone of influence of resistivity ρ . At a distance α of a

point in the medium from the point source, the surface area of the hemispherical shell is $2\pi\alpha^2$ of a point such that the potential for the homogeneous half-space is

$$\Phi(\mathbf{r}) = \frac{\rho l}{2\pi\alpha} \dots 10$$

In the field, two current electrodes, the current source +1 and the sink -1 are usually utilized. The potential distribution is symmetrical about the vertical placed at the mid-point between the two current electrodes. The potential at an arbitrary point from a given pair of current electrodes is obtained by applying equation 10.

$$\Phi (r) = \frac{\rho I}{2\pi} \left(\frac{1}{\alpha_{K_1}} - \frac{1}{\alpha_{K_2}} \right) \dots 11$$

where α_{K_1} and α_{K_2} are respective distances from the first (source) and second source (sink) current electrodes to the arbitrary point.

Since the potential difference between two points is usually measured, the injecting electrodes could be utilized to measure the potential difference but the impact of the resistances between the subsurface and current electrodes is not known precisely (Cheng et al., 1990). Therefore, two potential electrodes are often dedicated to ensuring the detection of the response signal if J_I and J_2 are the dedicated potential electrodes (Figure 1), the potential difference between J_I and J_2 otherwise becomes

$$\Delta \Phi = \frac{\rho I}{2\pi} \left(\frac{1}{K_1 J_I} - \frac{1}{K_1 J_2} - \frac{1}{K_2 J_1} + \frac{1}{K_2 J_2} \right) \dots 12$$

Berkeley Journal of Entomology and Agronomy Studies

Equation 12 is the observed potential over a homogeneous half-space with a typical four electrode configuration. Since the subsurface is typically homogeneous, the observed resistivity is expected to be apparent which serves as the resistivity of a homogeneous subsurface medium that would give the same resistivity value for the same field array. Apparent resistivity can be viewed as a weighted mean of the resistivity of the subsurface volume under the four electrodes (Aizebeokhai, 2010). The apparent is highly dependent on how the electrodes are configured and can be determined by the injection of current I and voltage $\Delta\Phi$. Therefore, the apparent resistivity is expressed as

$$\rho_a = F \frac{\Delta \Phi}{I} \dots 13$$

The geometric factor represented by F in equation 13 is dependent on how the electrodes are configured and it is expressed as

$$F = 2\pi \left(\frac{1}{K_1 J_I} - \frac{1}{K_1 J_2} - \frac{1}{K_2 J_1} + \frac{1}{K_2 J_2} \right) \dots 14$$

Solute Transportation is a function of contaminant flow. As contaminant flows through a pervious medium, dilution of the contaminant is observed as a result of the process called dispersion. If the concentration of the observed contaminants at a point source is C_{C_0} , then the concentration, $C_{T,L}$ after time, t at a distance L covered from that source as expressed by Ogata, 1970 and reported by Aweto et al., 2023.

$$C_{T,L} = \frac{c_{C_0}}{2} \left[F_{CE} \left(\frac{L - V_x t}{2\sqrt{D_L t}} \right) + exp \left(\frac{V_x t}{D_L} \right) F_{CE} \left(\frac{L + V_x t}{2\sqrt{D_L t}} \right) \right] \dots 15$$

Where F_{CE} represents the function of complementary error, D_L represents longitudinal coefficient of dispersion and V_{x} represents the mean linear velocity of groundwater. Equation 15 was employed to model the concentration of cyanide in the CME at different distances in meters (m) away from the cassava processing site.

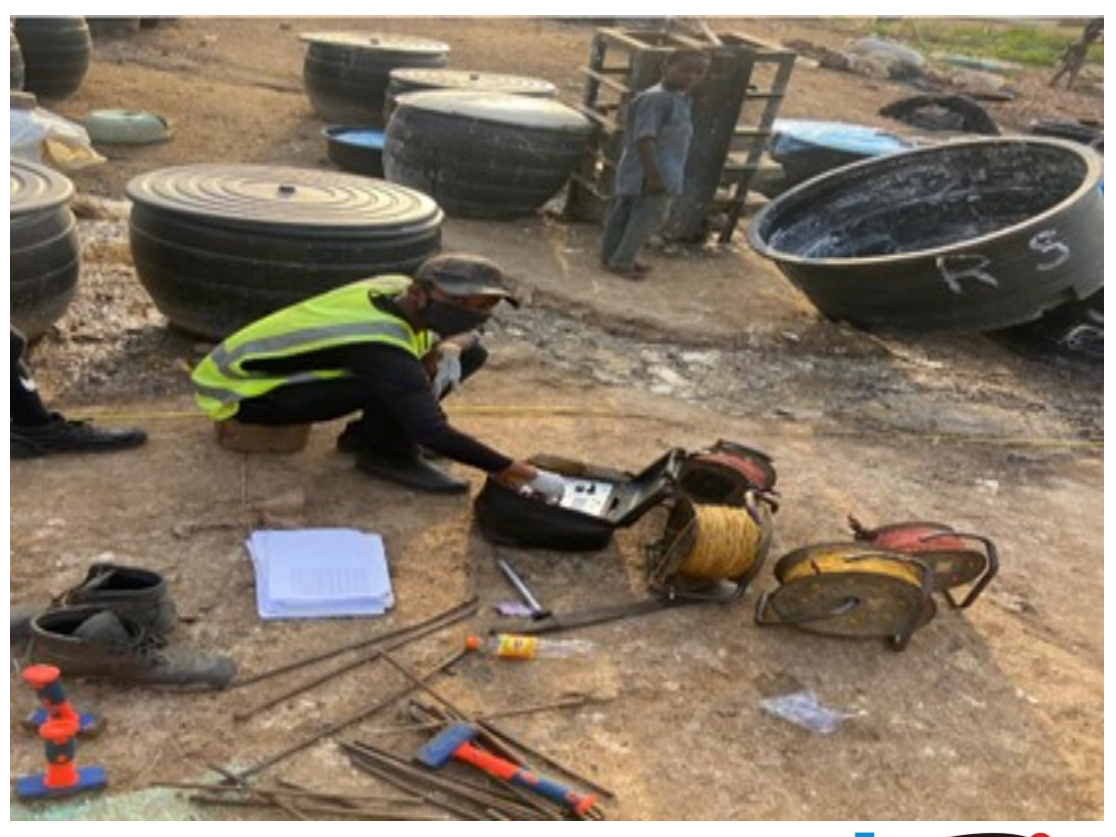
Field Operations and Data Acquisition

Earth Resistivity Meter (Campus-Ohmega Terrameter 0017model) was utilized for the 2D Electrical resistivity imaging and Vertical Electrical Soundings (VES). It consists of a transmitter unit for introducing current into the ground and a receiver unit for measuring the resulting potential difference. This geophysical instrument captures a series of resistivity values over multiple cycles and then averages them to obtain a final resistance value. Other field accessories used were a twelve-volt (12V) car battery, Hammer, Four (4) sets metallic electrodes, connecting cables and wires, A 100m measuring tape, Handheld GPS and a field

Vol. 8, No. 1

Berkeley Journal of Entomology and Agronomy Studies

notes and a writing pen were used to record the acquired field data. A survey was conducted to measure the electrical resistivity along five traverses, each with a spread length of 50 meters, using 2D electrical imaging and VES techniques (Figure 7 and 8). The measurements were gathered by configuring 2D electrical profiles using Campus-OhmegaTerrameter to create a 3D view using ZONDRES3-D Software. These procedures aimed to uncover the subsurface lateral and vertical variation of resistivity values by establishing the 3D sections on the cassava processing site. Wenner array was adopted due to its superior depth of investigation, favorable horizontal resolution, and comprehensive data coverage (Koefoed, 1979). The data acquisition involved a minimum electrode spacing of 2m. The 100m tape was reeled out laterally and both ends were nailed down at a fixed point. The positioning of the traverses was determined by the available space surrounding the Cassava processing site which covers about 0.17327km² (Figure 6). Hence, a total spread of 50m was established. The earth resistivity meter (CAMPUS-Ohmega Terrrameter) was positioned around the central point of the established 50m spread. Well-insulated cables and wires of sufficient length were used to connect the terminals of the earth resistivity meter to the four (4) metallic electrodes and were also used in connecting the earth resistivity meter to the power source.



BERKELEY RESEARCH & PUBLICATIONS INTERNATIONAL Bayero University, Kano, PMB 3011, Kano State, Nigeria. +234 (0) 802 881 6063, berkeleypublications.com



Berkeley Journal of Entomology and Agronomy Studies



Figure 7: Field Outline and Equipment Set-Up in Apete Cassava Processing Site

At constant probe spacing, the generated currents from the power source were introduced into the ground by hammering down the two (2) current electrodes to measure the electrical properties of the subsurface, and the resulting voltage difference was measured at the potential electrode. The resulting resistance values were displayed on the screen of the earth resistance meter. Precise coordinates of the measurement locations were captured using GPS. To obtain a comprehensive understanding of the resistivity variation with depth, three (3) VES were obtained along the five (5) traverses with a total spread of 70m, employing the Schlumberger electrode array to facilitate maximum current penetration into the subsurface. The current electrode spacing (AB) ranged from a minimum of 2.0m maintaining a maximum profile length of 50m each. Sounding points were strategically designated at 2m, 4m, 6m, and 8m intervals along the established five (5) traverses (4 traverses within the cassava processing site and 1 traverse at the control site); 40m away from the investigated area. Both surveys were repeatedly carried out for the purpose of making up a five level survey (n



Berkeley Journal of Entomology and Agronomy Studies

= 1, 2,5) and (na = 5, 10,... 25m) for first and second survey respectively. The resulting resistance values were multiplied with the geometric factor for each configuration to obtain the apparent resistivity values which were further analyzed and processed using the ZONDRes3D resistivity and IP inversion software to generate the inverted 3-D resistivity models. Inversion was undertaken in order to generate the electric resistivity structure of the subsurface which were then interpreted along their respective X, Y and Z directions to map the leachate plume beneath the cassava mill effluent (CME) site (Figure 8).

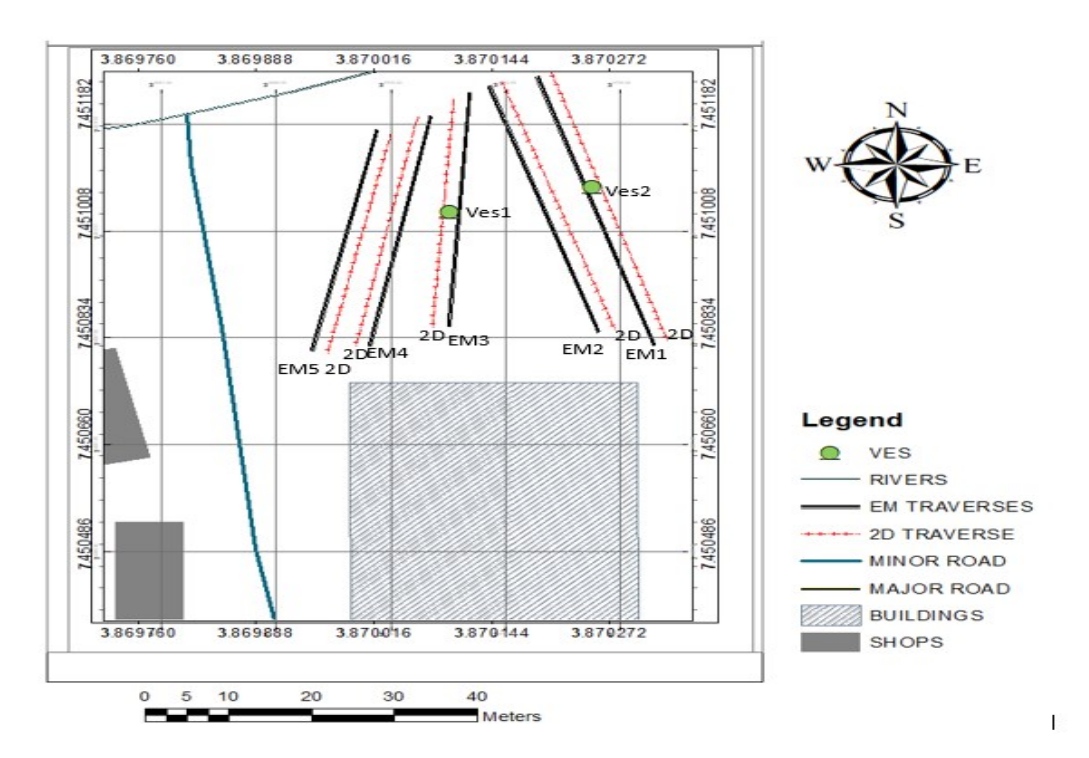


Figure 8: Basemap showing Data Location Points in the Study Area

Data Processing and Interpretation

The recorded data are inverted using the ZONDRES3-D inversion algorithm, developed in the 21st century, to yield a 3D resistivity distribution model of the subsurface. This is achieved through the use of the mesh constructor subroutine of ZONDRE3-D, which calculates theoretical apparent ground resistivity values. Additionally, the forward problem is computed before running the inversion. The resulting 3D inverse resistivity model is then smoothed to generate a comprehensive distribution of ground resistivity across the study area. The 3D resistivity image produced directly corresponds to the subsurface geologic layers. Consequently, the analysis and interpretation of the resistivity models were based on the geological knowledge of the study area. In performing the analysis and interpretation of

Berkeley Journal of Entomology and Agronomy Studies

the 3D resistivity image, careful attention is given to the electrical resistivity values, rather than the color representation, as each profile employs the same color while in data visualization; outcomes ZONDRE3-D were then presented through pseudosections or graphs for each survey line as 3-D modeling block.

The method adopted for the interpolation of the 2D resistivity sections into 3D resistivity displays was the inverse distance method where the 3D model produced aimed to view the distribution of leachate-contaminated soil in a more comprehensive pattern. An isosurface boundary was made between the suspected contaminated and non-contaminated soils from the results of the 3D model interpolation to see the distribution of subsurface leachate contamination; this has been carried out successfully in (Helene et al., 2020) and (Naim and Aprianto, 2016; Muhandi et al., 2020). The standard resistivity value used for the very low resistivity isosurface was $10~\Omega m$ (Naim and Aprianto, 2016; Soeryamassoeka et al., 2023).

Hydrogeochemical Analysis

In addition to the acquisition of the geoelectrical data, water samples were randomly collected at the five (5) cassava mill effluent location points strategically located and still operational in the study area (ApeteCME₁ to ApeteCME₅) and five (5) existing hand-dug well location points (ApeteWW₁ to ApeteWW₄) around the vicinity of Apete cassava processing site and ApeteWW₅ at control-site, 40m outside the vicinity of the cassava processing site across traverse 5); all within the study area. The collected water samples were transported to the Central Laboratory Obafemi Awolowo University, Ibadan Campus to determine hydrogeochemical concentrations basically Cyanide (CN) concentrations, the physicochemical parameters namely pH, Electrical conductivity, Total Dissolved solids, and heavy metals cum potential toxic elements using Atomic Absorption Spectrophotometer (AAS) equipment. This parameter was utilized in determining the spread of leachates in the investigated area. In addition, this data was further harnessed for validating the model outcomes and interpretations of the acquired 2D and 3D resistivity sections in the study area. Water level measurements were conducted alongside the water sample collections on the identified hand-dug wells within the study area following standard procedures for the purpose of determining the extent of leachate spread and validating the obtained 3D resistivity model sections across the study area.

Results and Discussion

Interpretation of 3D Resistivity Imaging

The resulting inverted resistivity model generated for the obtained data was presented and systematically interpreted thus about vertical and horizontal direction slicing to reveal the resistivity variation in the study area. However, the interpretation is typically based on three directional slice cuttings (X, Y and Z). The 3D resistivity image produced directly corresponds





Berkeley Journal of Entomology and Agronomy Studies

to the subsurface geologic layers. Consequently, the analysis and interpretation of the resistivity models were based on the geological knowledge of the study area. In performing the analysis and interpretation of the 3D resistivity image, careful attention is given to the electrical resistivity values, rather than the color representation, as each profile employs the same color. The inverted 3-D models generated revealed the presence of four basic lithologies in the weathered zone which consists of the clayey layer $(0\Omega m$ -14 Ωm), the sandy-clayey layer $(15\Omega m$ -49 Ωm), the weathered basement $(50\Omega m$ -79 Ωm), and the fresh basement rock $(80\Omega m$ - 200 Ωm) within the study area. The model shows the subsurface in three (3) orthogonal directions x-axis which shows the length, y-axis which shows the breadth and z-axis which shows the depth.

3-D Interpretation of Apete along Depth Z direction.

The horizontal view of the area, representing a full section at a depth of 0 meters and depicting the study area from the top surface, generally shows a thick concentration of leachate at the top. This concentration tends to decrease drastically with increasing depth. Leachate is dominant at the surface in both the western and eastern halves of the area but is less prominent in the central region. In addition to the leachate dominance, some parts of the cassava soil are slightly contaminated, where the leachate has not yet reached the surface. This depth indicates the presence of leachate and suggests a very low resistivity in these areas, ranging from 3 to 14 Ω m, due to high contamination (Figure 9).

At a depth of 2 meters, there is a significant reduction in the concentration of leachate (indicated by the blue color zone), and its distribution at this level is much more limited. Leachate is mostly confined to minor traces around the central part of the area. Major portions of the area are only slightly contaminated, suggesting that leachate is gradually approaching these regions and indicating low resistivity. At this depth, the resistivity ranges from 9 to 50 Ω m (Figure 10). The iso-resistivity structure at a depth of 4 meters shows that leachate has been completely removed from the soil at this depth, with no traces remaining. The western half of this segment shows slight to partial contamination with low resistivity, indicating that the leachate plume is likely to reach this area soon. Conversely, the eastern half (indicated by the red portion) exhibits very high resistivity; it is free from contamination. The general resistivity at a depth of 4 meters ranges from 32 to $100 \Omega m$ (Figure 11). The isoresistivity structure at a depth of 6m illustrates that the soil at this level shows little to no contamination. The eastern portion of the structure is completely free from contamination, while the western half is only minimally contaminated, approaching a state of being nearly free from leachate. There are no detectable traces of leachate at this depth. This level exhibits higher resistivity compared to the previous depths, with resistivity values ranging from 50 to 200 Ω m (Figure 12). The iso-resistivity profile at a depth of 8m reveals that the western half of the structure shows slight contamination, indicating that the migrating plume has yet



Berkeley Journal of Entomology and Agronomy Studies

to reach this area, though only a small portion of it. The eastern half is free from contamination and dominates the major portion of the surface at this depth. This area exhibits high resistivity due to the lack of contamination (indicated by the red/purple color zone), with resistivity values ranging from 55 to 200 Ω m (Figure 13). At a depth of 10m, the structure shows little to no contamination. Most regions are free from contamination, particularly the eastern half of the structure, which exhibits high resistivity. The western half has only a small portion that is slightly contaminated. Leachate is absent in this region, and the plume is still migrating but has not yet reached this depth (Figure 14).

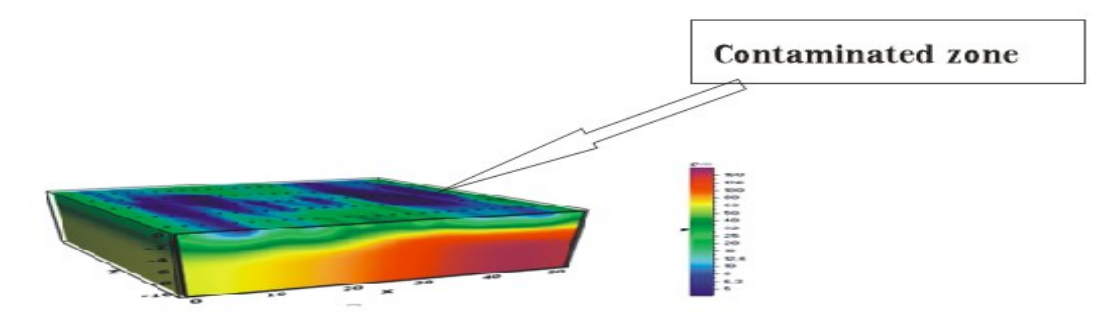


Figure 9: 3-D Geo-electric view of the study area at depth slice 0m on the Z-axis

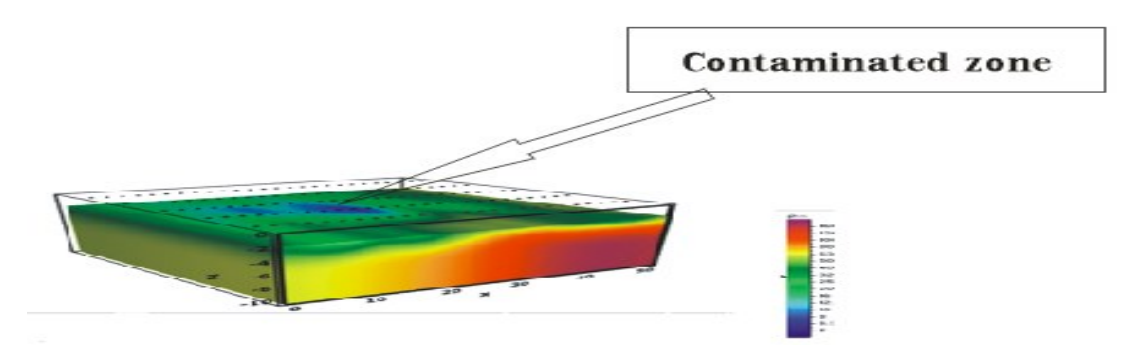


Figure 10: 3-D Geo-electric view of the study area at depth slice 2m on the Z-axis

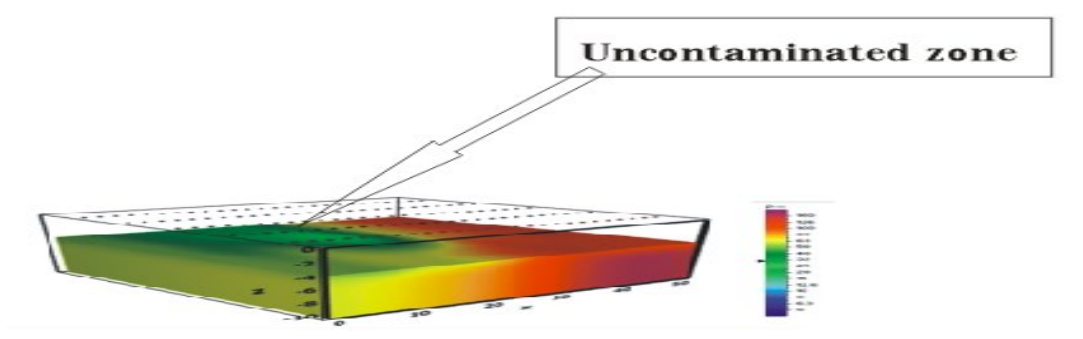


Figure 11: 3-D Geo-electric view of the study area at depth slice 4m on the Z-axis

BERKELEY RESEARCH & PUBLICATIONS INTERNATIONAL Bayero University, Kano, PMB 3011, Kano State, Nigeria. +234 (0) 802 881 6063, berkeleypublications.com



E-ISSN 3027-2157 P-ISSN 3026-9482

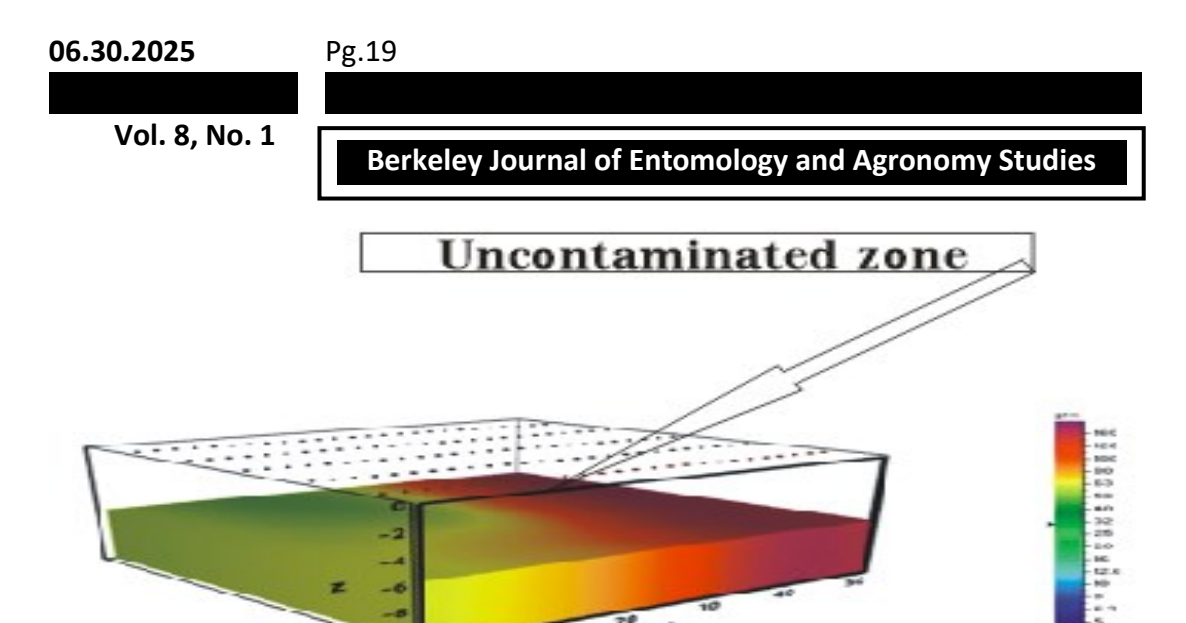


Figure 12: 3-D Geo-electric view of the study area at depth slice 6m on the Z-axis

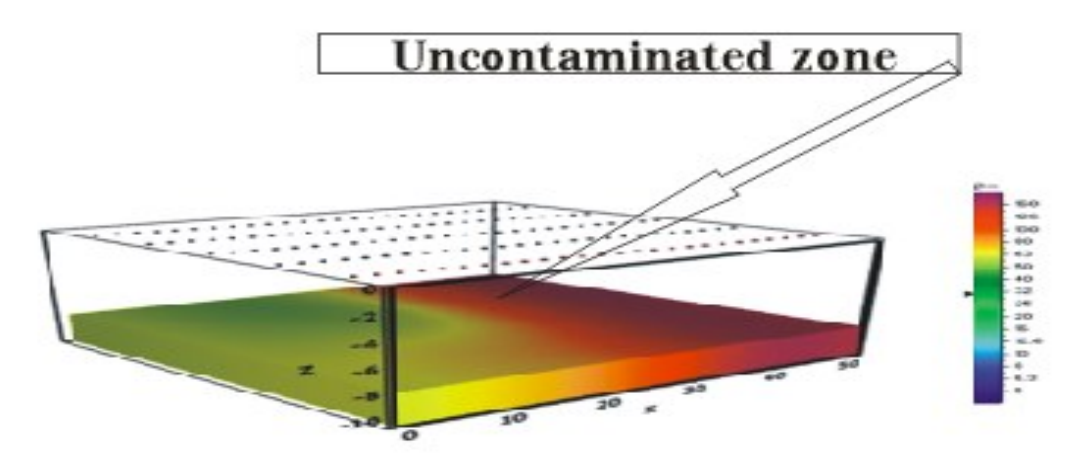


Figure 13: 3-D Geo-electric view of the study area at depth slice 8m on the Z-axis

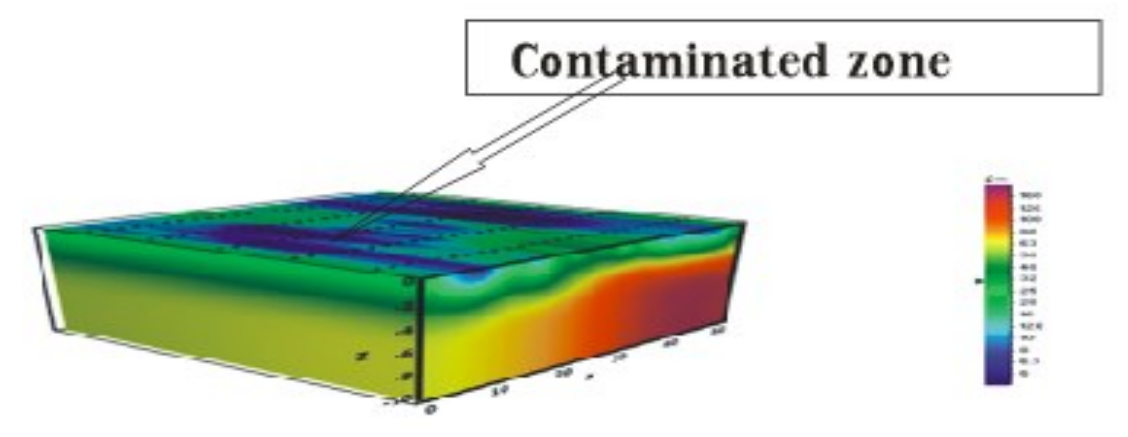


Figure 14: 3-D Geo-electric view of the study area at depth slice 10mon the Z-axis



Berkeley Journal of Entomology and Agronomy Studies

3-D Interpretation of Apete along Depth X Direction.

The iso-resistivity profile at 0m along the X-axis reveals a slightly contaminated portion at the upper part, characterized by low resistivity. The major and dominant area located in the lower zone of the structure is also slightly contaminated, though less so compared to the upper part. The lower zone exhibits higher resistivity than the upper zone. The overall resistivity at this depth along the X-axis ranges from 32 to 62 Ω m (Figure 15). The isoresistivity profile at 10m along the X-axis shows leachate intrusion in the upper part of this zone, characterized by low resistivity. Below the leachate-affected area, there is a region of slight contamination, indicating that the plume has yet to migrate into this area. The major dominant zone, located further downwards in the southern half of the structure, is also slightly contaminated and exhibits low resistivity, though higher than the upper zone. At this depth, resistivity ranges from 8 to $60 \Omega m$ (Figure 16). The iso-resistivity profile at 20 meters along the X-axis highlights leachate intrusion in the central part of the upper half of the structure. Leachate is present from approximately 0 to 2 meters in a small portion of the middle part of the upper half. Consequently, this upper region exhibits low resistivity, which increases with depth. The mid-region of the subsurface structure (indicated by the green zone) shows slight contamination suggesting that the migrating plume has not yet reached the area. In contrast, the eastern part of the lower zone (indicated by the red color) exhibits high resistivity, indicating that it is free from contamination (Figure 17).

The topmost region at 30 meters along the X-axis shows leachate intrusion from the upper surface, primarily affecting the middle portion of the upper part (one-quarter of the view). Below this leachate-affected area, the topmost region is slightly contaminated, indicating that the plume has not yet migrated there. The lower half of the view exhibits high resistivity. with the eastern part of the downward zone being free from contamination. In contrast, the western half of the downward region remains slightly contaminated. Overall, the downward zone has higher resistivity compared to the upper part of the structure (Figure 18). The isoresistivity profile at 40 meters along the X-axis shows leachate intrusion in the topmost region of the upper part of the zone, affecting approximately one-sixth of the entire area. Below this leachate zone is a region that is slightly contaminated, indicating that the plume has not yet reached this area. The resistivity of the upper zone ranges from 6 to 63 Ω m. The downward zone, which comprises about four-sixths of the entire area, is free from contamination and exhibits high resistivity, especially with increasing depth. The resistivity of this downward zone ranges from 100 to 220 Ω m (Figure 19). The iso-resistivity profile at 50 meters along the X-axis shows an absence of leachate at this depth. Consequently, the upper region contains slightly contaminated soil, comprising approximately one-quarter (1/4) of the entire view. The downward zone, which dominates around three-quarters (3/4) of the entire view, is free from contamination and thus exhibits very high resistivity (Figure 20).



Berkeley Journal of Entomology and Agronomy Studies

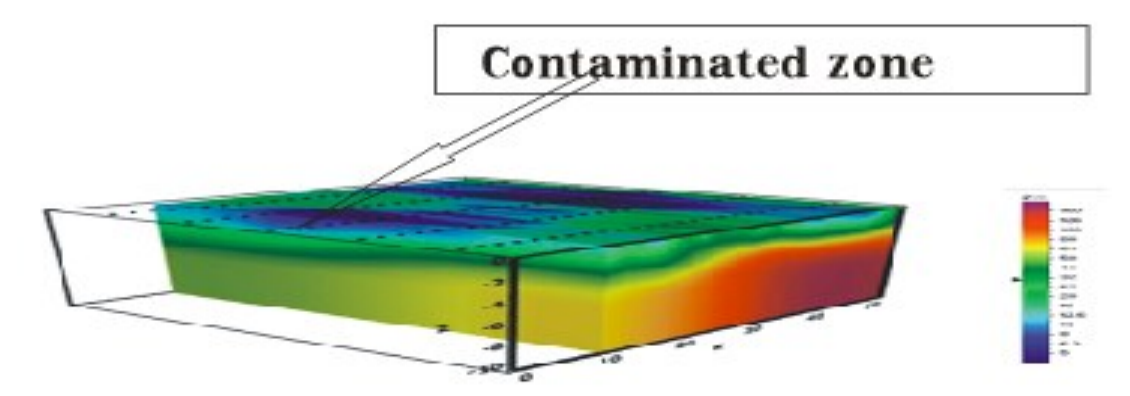


Figure 15: 3-D Geo-electric view of the study area at depth slice 0m on the X-axis

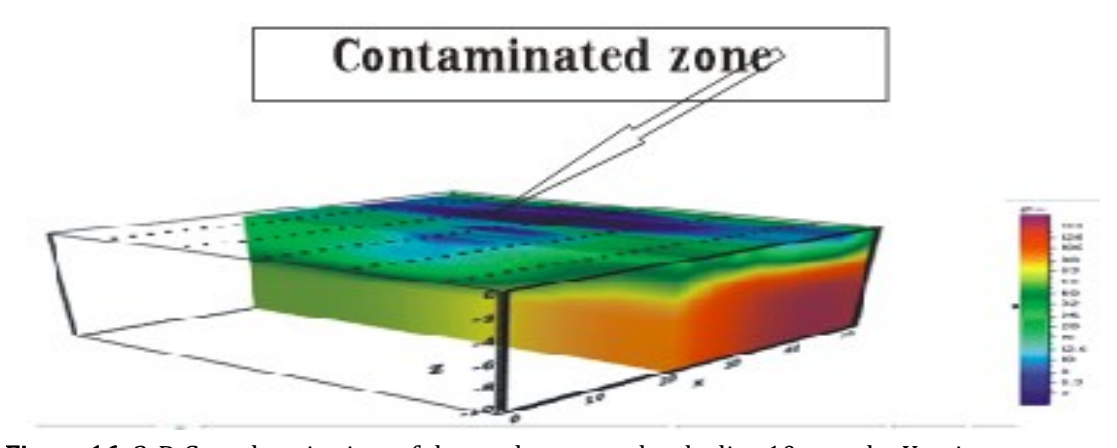


Figure 16: 3-D Geo-electric view of the study area at depth slice 10mon the X-axis

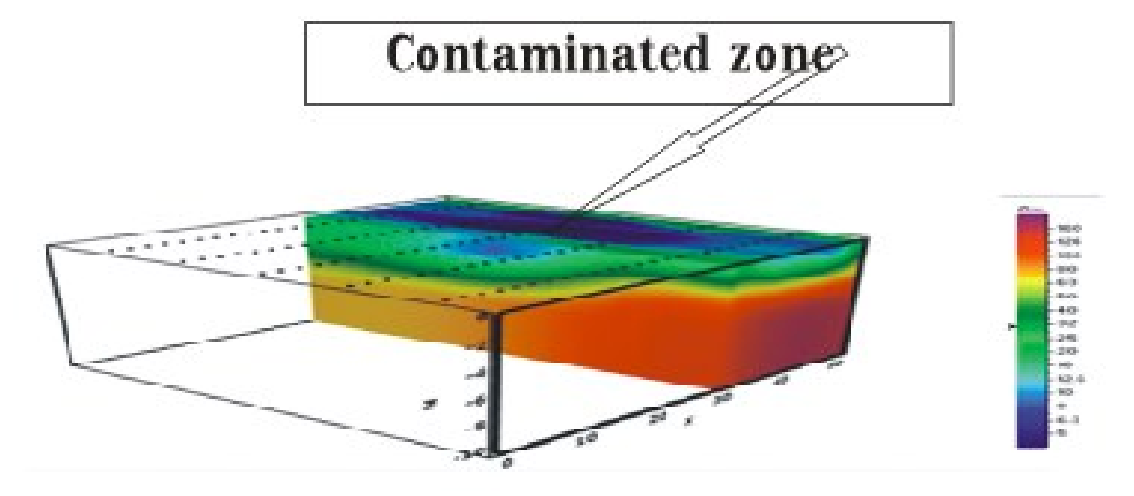


Figure 17: 3-D Geo-electric view of the study area at depth slice 20mon the X-axis



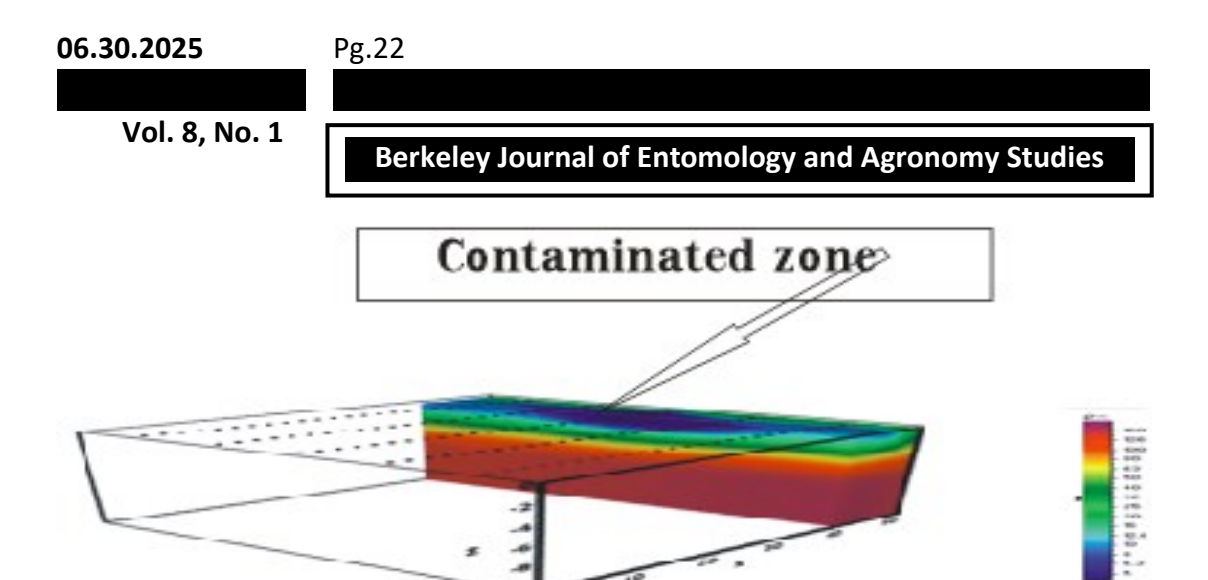


Figure 18: 3-D Geo-electric view of the study area at depth slice 30m on the X-axis

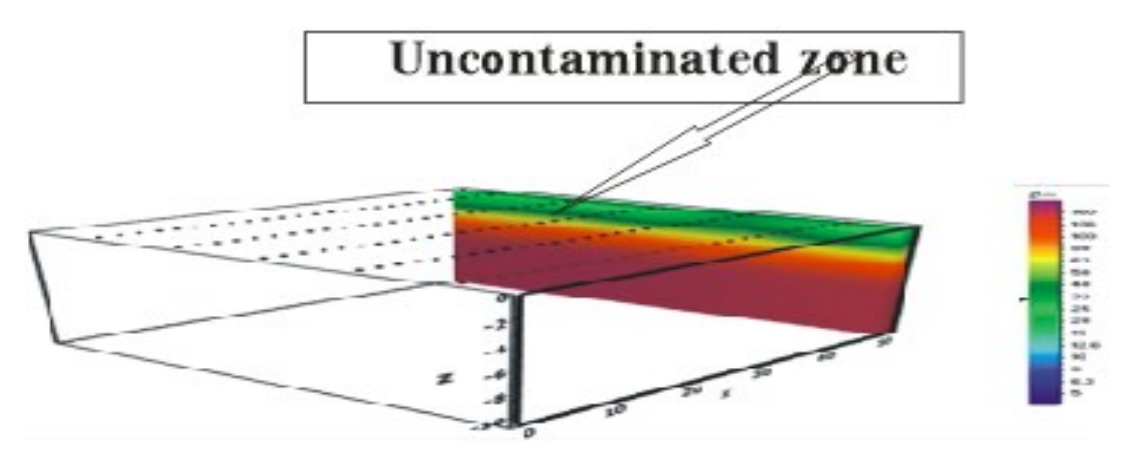


Figure 19: 3-D Geo-electric view of the study area at depth slice 40m on the X-axis

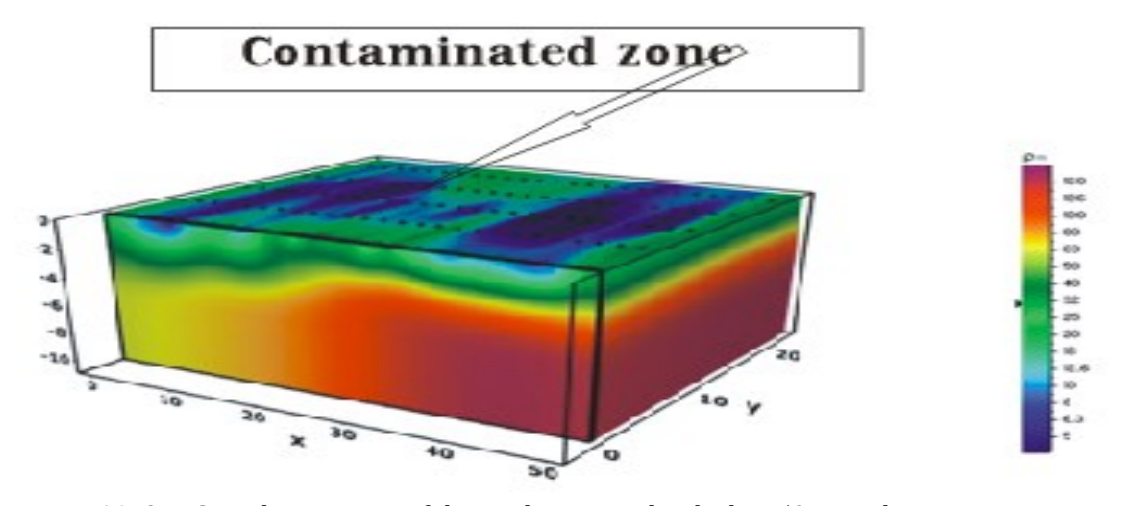


Figure 20: 3-D Geo-electric view of the study area at depth slice 50m on the X-axis



Vol. 8, No. 1

Berkeley Journal of Entomology and Agronomy Studies

3-D Interpretation of Apete along Depth Y Direction.

At a depth of 0 meters, the iso-resistivity structure shows leachate intrusion from the topsoil into the upper portion of this section, affecting only a small area. The section moving downward contains a zone that is slightly contaminated, indicating that the plume has not yet reached this area. The downward region dominating approximately three-quarters (3/4) of the entire view exhibits higher resistivity when compared to the upper section. The southern view is divided into two parts: the eastern segment and the western segment. The western region is slightly contaminated but has a higher resistivity than the upper section, while the eastern segment exhibits very high resistivity due to its lack of contamination (Figure 21).

The iso-resistivity structure at 5 meters along the Y-axis shows leachate intrusion from the topsoil into the upper portion of this section, affecting only a small area. The section below this upper portion contains a zone that is slightly contaminated, indicating that the plume has not yet reached this area. The resistivity of the upper region ranges from 7 to 40 Ω m. The downward region comprising of approximately three-quarters (3/4) of the entire view, exhibits higher resistivity when compared to the upper section. The southern view is divided into two parts: the eastern segment and the western segment. The western region is slightly contaminated but has a higher resistivity than the upper section, while the eastern segment shows very high resistivity due to its lack of contamination (Figure 22). The structure at 10 meters along the Y-axis shows that leachate intrudes into the upper half of the zone, affecting a large portion up to a depth of approximately 3 meters. Below this area, there is a region that is slightly contaminated, indicating that the migrating plumes have not yet reached it. The downward zone, which comprises about two-thirds (2/3) of the entire area, is divided into the eastern and western regions. The western region is slightly contaminated and has low resistivity, though it is higher than that of the upper zone. The eastern region is free from contamination and exhibits high resistivity, with values ranging from approximately 90 to $210~\Omega m$ (Figure 23). At a depth of 15 meters, the iso-resistivity structure reveals leachate intrusion into the upper layer of the structure. The middle portion extending westward into the downward zone is slightly contaminated and exhibits low resistivity. In contrast, the eastward section of the downward zone is free from contamination, resulting in high resistivity (Figure 24). At a depth of 20 meters, the iso-resistivity structure is predominantly characterized by a slightly contaminated zone (indicated by the green/yellow zone), which covers approximately 70% of the entire view and exhibits low resistivity. The topmost edge of the upper zone shows minor leachate intrusion in a very small quantity. The eastern half of the downward zone is free from contamination, resulting in high resistivity (Figure 25).

3-D Interpretation of Apete showing a model from beneath



Berkeley Journal of Entomology and Agronomy Studies

The iso-resistivity structure viewed from below reveals that the zone is divided into two regions based on resistivity and contamination: the eastern region and the western region. The structure beneath this zone shows no presence of leachate. However, the western portion of the zone is slightly contaminated but still exhibits higher resistivity compared to the topmost and upper zones. The dominant eastern region, which covers the majority of the area, has high resistivity and is free from contamination (Figure 26).

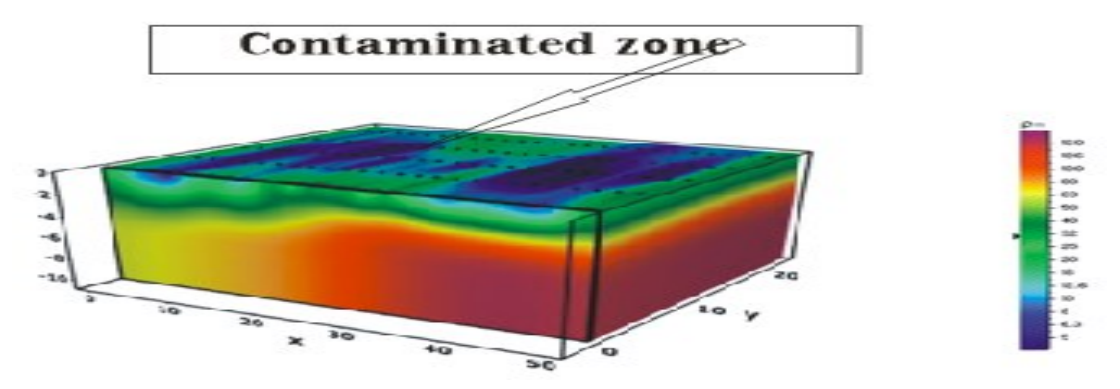


Figure 21: 3-D Geo-electric view of the study area at depth slice 0m on the Y-axis

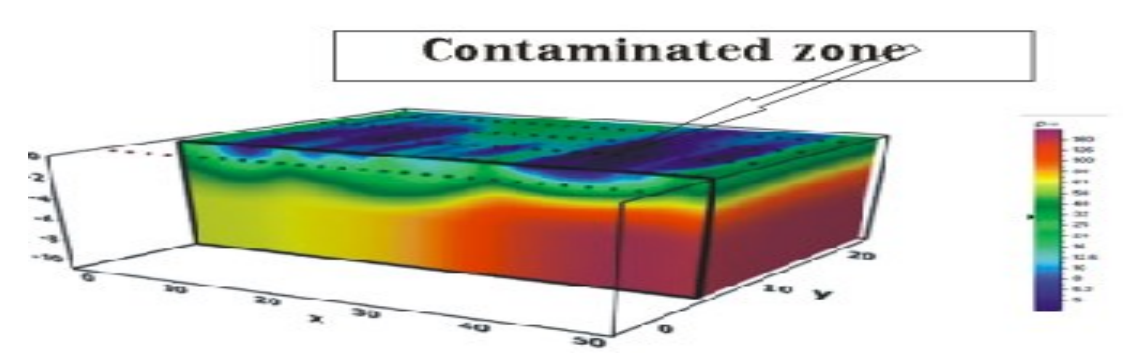


Figure 22: 3-D Geo-electric view of the study area at depth slice 5mon the Y-axis

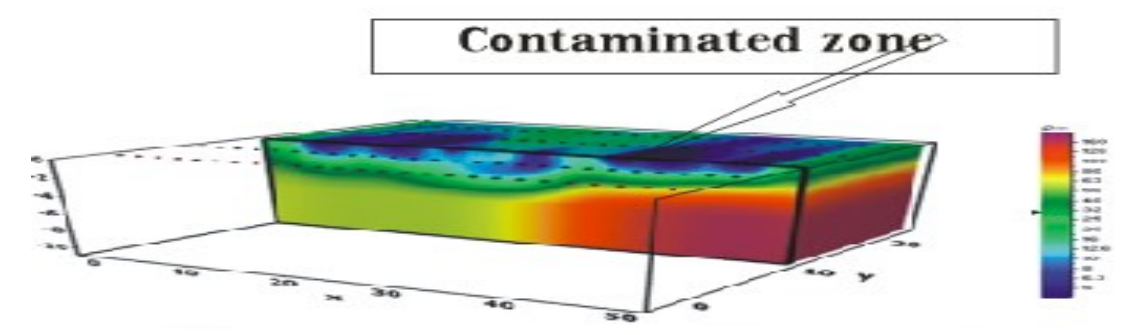


Figure 23: 3-D Geo-electric view of the study area at depth slice 10m on the Y-axis

BERKELEY RESEARCH & PUBLICATIONS INTERNATIONAL Bayero University, Kano, PMB 3011, Kano State, Nigeria. +234 (0) 802 881 6063, berkeleypublications.com



E-ISSN 3027-2157 P-ISSN 3026-9482

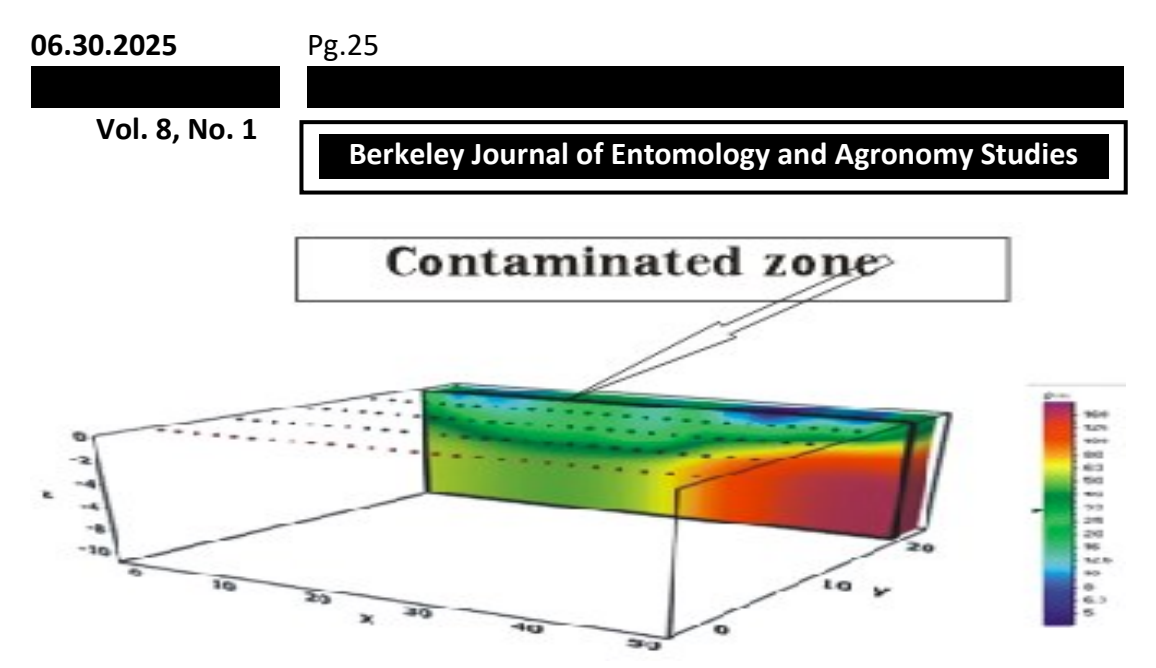


Figure 24: 3-D Geo-electric view of the study area at depth slice 15m on the Y-axis

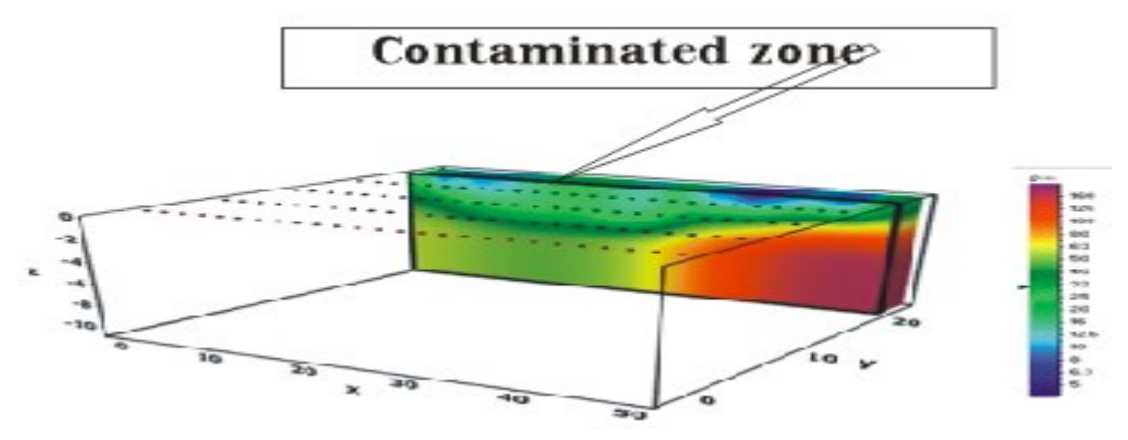


Figure 25: 3-D Geo-electric view of the study area at depth slice 20m on the Y-axis

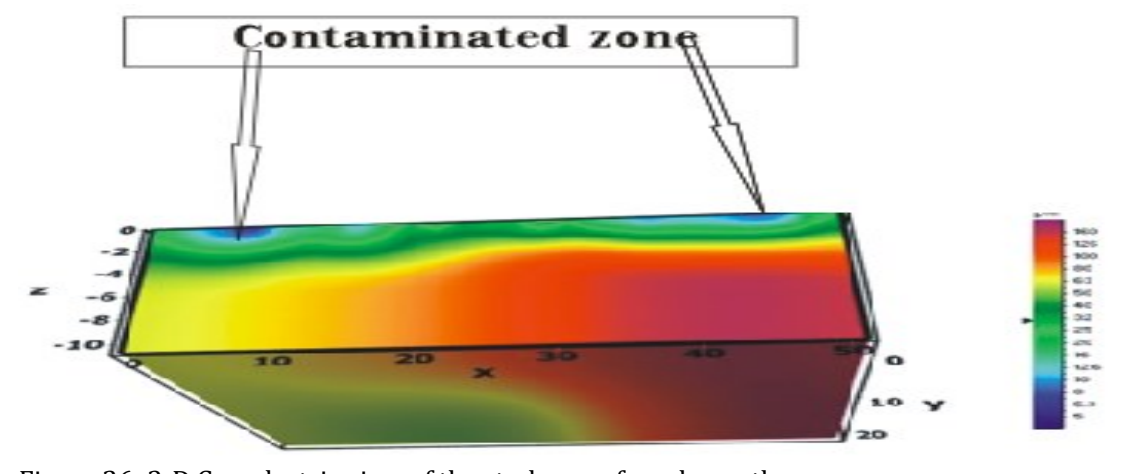


Figure 26: 3-D Geo-electric view of the study area from beneath



Berkeley Journal of Entomology and Agronomy Studies

3-D Interpretation of Apete Showing a cross-cutting direction.

The cross-sectional view shows the northern, southern, western, and eastern aspects of the iso-resistivity structure. The northern view (upper zone) reveals leachate intrusion from the topsoil, which extends to a depth of approximately 2.5 meters before vanishing. The leachate is predominant between 0 and 2.5 meters in the structure. Below the leachate-affected region, the western view shows a zone that is slightly contaminated. Moving from the middle region to the eastern region, the area is free from contamination and exhibits high resistivity (Figure 27).

From this view, the eastern section shows that the upper layer contains leachate, followed by a region that is slightly contaminated, indicating that the migrating plume has not yet reached this area and remains in the upper region. The dominant zone, extending from the upper region to the lower half of the downward zone, exhibits high resistivity and is free from contamination. The western view also shows leachate at the top, but the remaining downward region is slightly contaminated. This westward section is characterized by low resistivity (Figure 28).

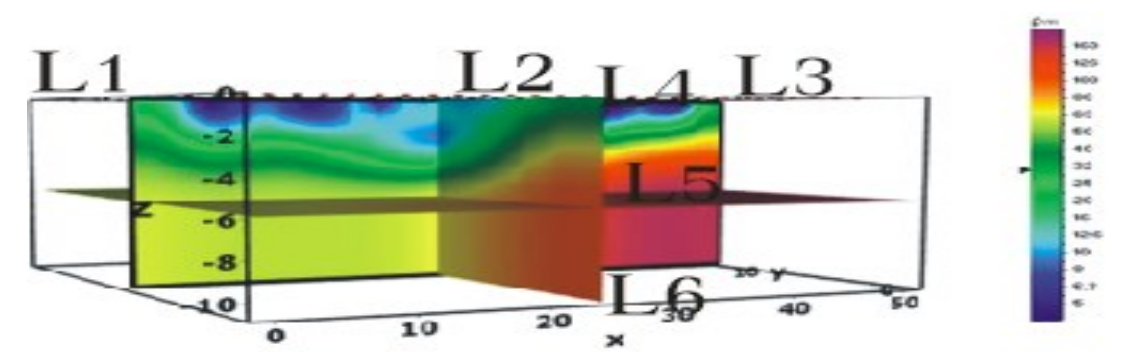


Figure 27: 3-D Geo-electric view of the study area showing a cross-cutting direction

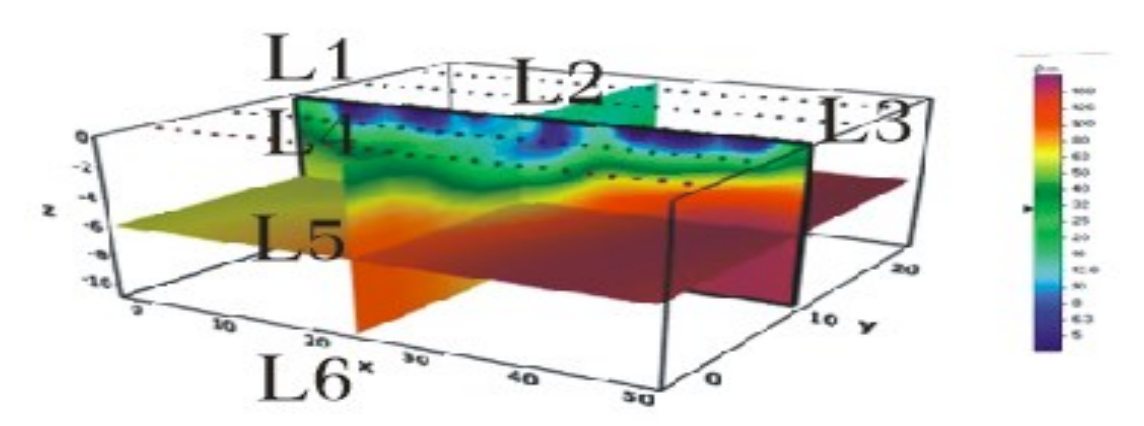


Figure 28: 3-D Geo-electric view of the study area showing a cross-cutting direction

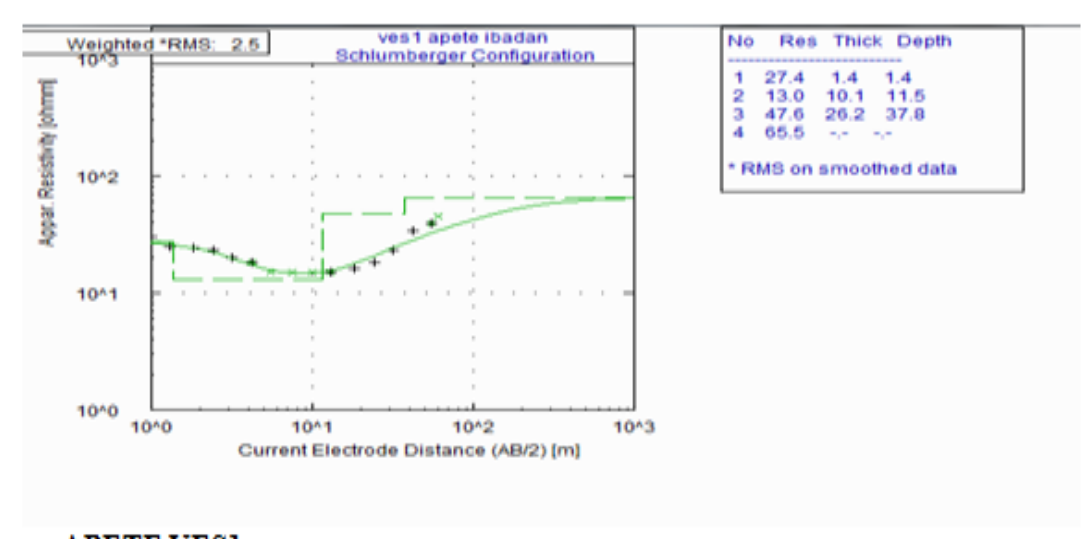


Berkeley Journal of Entomology and Agronomy Studies

Since the 2D resistivity is a depiction of the layers beneath the cassava processing site and the resistivity cross-sections of the resistivity lines L1 to L6 were combined to form a 3D cross-section. Aside from the 3D resistivity model describing the subsurface layers within the investigated area; it also shows the direction of the leachate spreading from the cassava processing site. In figure 27 and 28, the resistivity values on track lines L5 and L6 were greater than that on L1, L2, L3 and L4 because the lines extended through a dry soil away from the CME effluents passing over at a distance of 0 to 70m. The resistivity values of the dry soil free of CME leachates were greater than that of the wet soil full of concentrated CME leachates. During the field investigation, it was visible on the surface that this track lines were dry resulting to a higher resistivity value making it less effective at conducting electricity.

Interpretation VES Geo-Resistivity Sections

Three (3) vertical electrical soundings were established in the study area alongside the 3D electrical resistivity imaging to comprehensively understand the resistivity variation and thickness with depth across the study area. The results of the established three (3) vertical electrical soundings are presented in Table 1 and it shows the thickness, depth, and resistivity of different geoelectric layers and their lithological sequence. Four (4) layers were identified in the study area with resistivities ranging from $13.0\Omega m$ to $65.5\Omega m$ (VES 1), $18.0\Omega m$ to $104.6\Omega m$ (VES 2), $103.8\Omega m$ to $340\Omega m$ (VES 3). These consist of topsoil, clayey sand, fractured basement, and fresh basement. The iterated curves obtained for the study area are presented in (Figure 29) revealing the H (p1>p2<p3), H (p1>p2<p3), and A (p1<p2<p3) vertical electrical sounding curve types; where p1, p2 and p3 are the resistivities of the first, second, and third layer respectively.



APETE VES1



Berkeley Journal of Entomology and Agronomy Studies

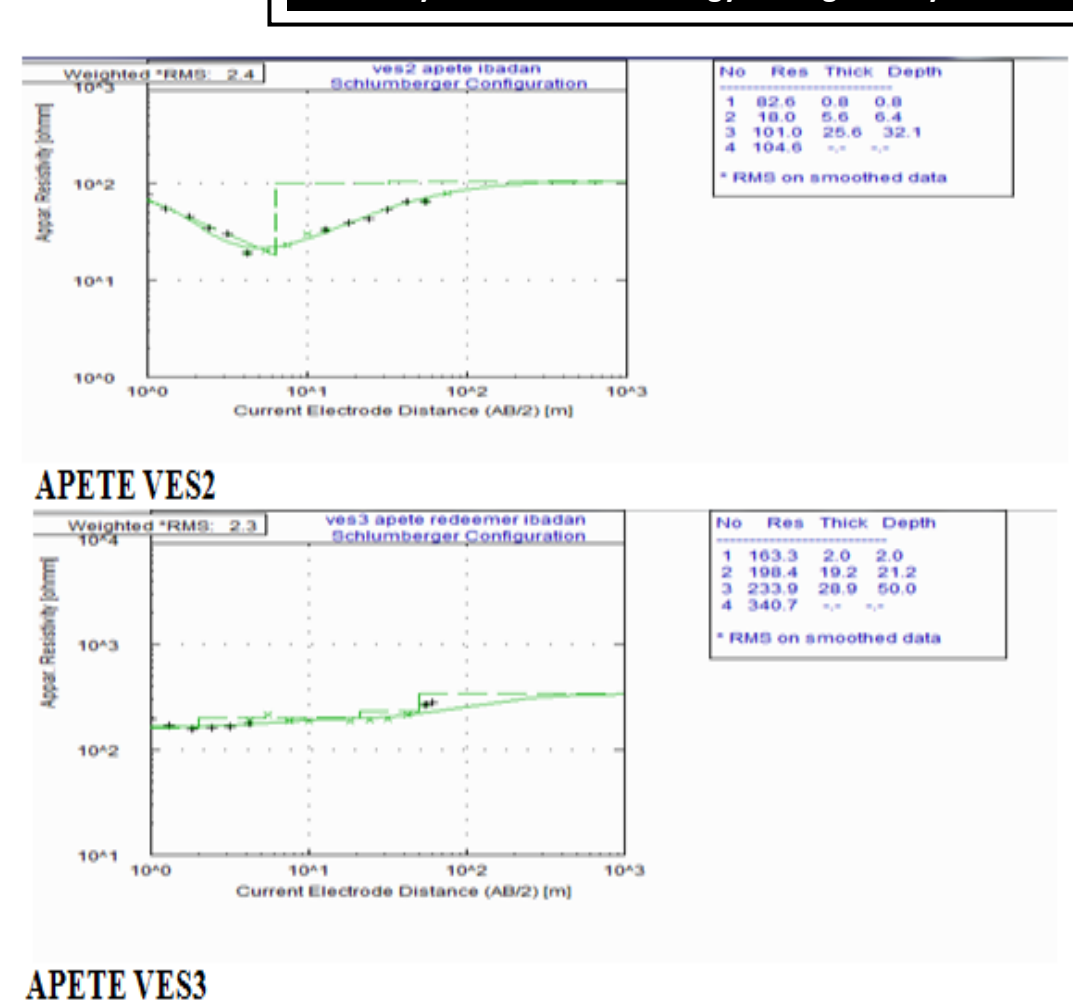


Figure 29: Iterated curves for APETE VES1, 2, and 3 (CONTROL Station)

Table 1: Lithological Table for the Established VES points

	Layer	Resistivity(Ω m)	Thickness(m)	Depth	Lithology Sequences	
APETEVES1	1	27.4	1.4	1.4	Topsoil	
	2	13.0	10.1	11.5	Contaminated zone	
	3	47.6	26.2	37.8	Partly low/ weathered/	
	4	65.5			Weathered/ partly	
APETEVES2	1	82.6	0.8	8.0	Top material	
	2	18.0	5.6	6.4	Contaminated/ sandy clay	
	3	101.4	25.6	32.1	Weathered layer	
	4	104.6			Fractured/partly fresh	
APETEVES3 (CONTROL)	1	103.8	2.0	2.0	Top lateritic	
	2	198.4	19.2	21.2	Clayey sand	
	3	233.1	28.9	50.0	Fractured	
	4	340.9			Fresh Basement	

BERKELEY RESEARCH & PUBLICATIONS INTERNATIONAL

Bayero University, Kano, PMB 3011, Kano State, Nigeria. +234 (0) 802 881 6063, berkeleypublications.com



E-ISSN 3027-2157 P-ISSN 3026-9482

Berkeley Journal of Entomology and Agronomy Studies

Interpretation of the Vertical Electrical Sounding at APETEVES1

VES 1 reveals four (4) geoelectric layers with resistivity values of $27.4\Omega m$, $13.0\Omega m$, $47.6\Omega m$, and $65.5\Omega m$ corresponding to topsoil, clayey, sandy, and fresh basement, respectively. The topsoil has a thickness of 1.4m and a depth of 1.4m. The second layer has a thickness of 10.1m and a depth of 11.5m. The third layer has a thickness of 26.2m and a depth of 37.8m and that of the last layer could not be determined. The curve type is an H curve type (Figure 29).

Interpretation of the Vertical Electrical Sounding at APETEVES2

VES 2 reveals four (4) geoelectric layers with resistivity values of 82.6m, 18.0m, 101.4m, and 104.6m corresponding to topsoil, sandy clay, weathered layer, and fresh basement, respectively. The topsoil has a thickness of 0.8m and a depth of 0.8m. The second layer has a thickness of 5.6m, and a depth of 6.4m, and the third layer has a thickness of 25.6m and a depth of 32.1m and that of the last layer could not be determined. The curve type is an H curve type (Figure 29).

Interpretation of the Vertical Electrical Sounding at APETEVES3 (Control Station)

VES 3 reveals four (4) geoelectric layers with resistivity values of 103.8m, 198.4m, 233.1m, and 340.9m corresponding to topsoil, clayey sand, fractured layer, and fresh basement, respectively. The topsoil has a thickness of 2.0m and a depth of 2.0m. The second layer has a thickness of 19.2m, and a depth of 21.2m, and the third layer has a thickness of 28.9m and a depth of 50.0m and that of the last layer could not be determined. The curve type is an A curve type (Figure 29). The findings of the Electrical Resistivity Imaging conducted on VES 1 and 2 revealed the presence of leachate infiltrations in the subsurface; indicated by low resistivity and high conductivity readings. These results suggest contamination of the respective layers both in APETEVES1and APETEVES2 (Table 1). Conversely, VES 3 which served as a control point displayed high resistivity and low conductivity value, signifying an absence of leachate migration and contamination in this area. This indicates that the area is relatively uncontaminated due to the large distance from the investigated area (about 200m).

Water Level Measurement and Geochemical Evaluations

The results of the conducted water level measurements as well as the geochemical analyses of CME and groundwater samples respectively collected from five (5) different waste-pits and hand-dug wells at varying distances from the traverse locations at Apete Cassava Processing site are presented in Table 2 and 3. The pH varied from 2.76 to 3.26 and 4.93 to 6.2 in CMEs and groundwater respectively. Izah et al., 2017 and Aweto et al., 2023 reported pH values less than 5.0 in CME. The pH of the effluent indicated it was acidic, and this was as a result of the presence of high hydrogen cyanide content in the CMEs. Total Dissolved Solids



Vol. 8, No. 1

Berkeley Journal of Entomology and Agronomy Studies

(TDS) varied from 10,206 mg/L (ApeteCME $_5$) to 21,500 mg/L (ApeteCME $_1$) and 60 mg/L (ApeteWW $_1$) to 255 mg/L (ApeteWW $_2$); the Electrical Conductivity (EC) was observed to range from 11,114 to 32,360 μ s/cm and 32 to 135 μ s/cm for CMEs and groundwater respectively. The cyanide (CN) concentration values were found to range from 7.19 mg/L (ApeteCME $_1$) to 31.25 mg/L (ApeteCME $_5$) and 0.00 to 0.03 (ApeteWW $_1$ and ApeteWW $_2$); Aweto et al., 2023 reported CN concentration values that ranged between 3.14 to 29.31 mg/L. The heavy metals exhibited concentration values that varied between 1.72 to 4.62 mg/L for CMEs and 0.009 to 0.02 mg/L for groundwater; 0.83 to 4.42 mg/L for CMEs and 0.00 to 0.13 mg/L for groundwater; 0.25 to 0.93 mg/L for CMEs and 0.001 to 0.004 mg/L for groundwater; 3.29 to 6.75 mg/L for CMEs and 0.03 to 0.26 mg/L for groundwater; 0.02 to 0.42 mg/L for CMEs and 0.00 to 0.02 mg/L; 0.38 to 3.11 mg/L and 0.00 to 0.021 mg/L; all were respectively recorded for Cu, Zn, Fe, Mn, Cd and Pb for both CMEs and groundwater sources of the study area (Table 1).

Table 2: Geochemical Evaluation of CME and groundwater at Apete Cassava Processing Site

Sampling Codes	CN	pН	EC	TDS	Cu ²⁺	Zn ²⁺	Fe ²⁺	Mn ²⁺	Cd ²⁺	Pb ²⁺
ApeteCME ₁	31.25	2.85	32,360	21,500	4.62	4.42	0.85	4.22	0.42	0.38
ApeteCME ₂	28.62	3.26	15,700	11,400	3.93	2.28	0.93	5.83	0.23	0.47
ApeteCME ₃	25.59	2.88	19,250	18,326	3.42	2.17	0.67	3.29	1.03	0.65
ApeteCME ₄	18.45	2.76	19,110	13,576	3.25	1.05	0.86	6.75	0.22	3.11
ApeteCME ₅	7.19	3.22	11,114	10,206	1.72	0.83	0.25	6.46	0.02	0.78
ApeteWW ₁	0.03	5.69	32	60	0.02	0.04	0.004	0.03	0.00	0.021
ApeteWW ₂	0.03	4.93	110	255	0.03	0.08	0.02	0.26	0.00	0.009
ApeteWW ₃	0.01	4.96	84	178	0.02	0.13	0.001	0.03	0.004	0.003
ApeteWW ₄	0.00	5.68	135	121	0.05	0.00	0.002	0.07	0.00	0.002
ApeteWW ₅	0.00	6.20	133	93	0.009	0.03	0.002	0.04	0.02	0.00
WHO	0.2	6.5 - 8.5	1000	500	2.0	4.0	0.30	0.1	0.003	0.01

Keys:

CMEWP = Cassava Mill Effluent collected from the Waste Pit.

WHO = World Health Organization from Drinking Water Standard

Table 3: Water Level Measurement at Anete

Table 3.	Water Lev	ei measure	illelli ai A	pete				
Well	Latitude	Longitude	Elevation	Well	Water	Water	WPD	CMED
code				Head	Level	Depth		
APWW1	7.451111	3.870278	190m	0.36m	3.34m	3.78m	43m from	15m from
							APWW2	traverse 01
APWW2	7.451389	3.870278	190m	Nil	0.84m	1.77m	35m from	21m from
							APWW3	traverse 02
APWW3	7.451667	3.870556	190m	0.5m	3.27m	3.91m	49m from	35m from
							APWW4	traverse 03
APWW4	7.450833	3.870278	190m	0.71	3.97m	4.60m	49m from	27m from
							APWW5	Traverse 04
APWW5	7.450701	3.870119	190m	0.5m	3.30m	4.22m	49m from	20m from
							APWW4	traverse 05



Vol. 8, No. 1

Berkeley Journal of Entomology and Agronomy Studies

Key

APWW= Apete Well Water

WPD = Well Proximity Distance

CMED = Cassava Mill Effluent Distance from the Investigated 2D traverses

All analyzed samples of CMEs possessed high concentration values of TDS, EC, CN, and constituents of heavy metals; this depicts that the encountered CME in the study area has tendency of migrating to the neighbouring groundwater system (Aweto et al., 2023). The presence of potential toxic elements cum heavy metals namely Pb, Fe and Mn in groundwater is attributable to the particles from abrasive activities of mechanical devices that formed parts of the cassava grinding machinery which inadvertently found their ways at different times via wearing and tearing stages, though quite unnoticed as the machine is progressively used. The observed low pH concentration has enhanced the solubility of the metals leading to about two-fold increment in absolute metal concentration. High concentrations of similar values were equally reported in CME within South-South Nigeria notably from Nwakanda et al., 2012, Igbinosa and Igiehin, 2015 and Igbinosa (2015). The reported levels of chemical parameters as observed from the groundwater samples were quite less in magnitude than those encountered in the CME₅. The current pH values (4.93 to 6.20 mg/L) is an indication of a typical acidic groundwater system depicting the dominant nature of acidity encountered in the groundwater might not entirely be related to CME effluent discharge because the shallow state of the existing wells can enhance the acidity increase (Etu-Efetor and Odigi, 1983; Aweto et al., 2023).

Furthermore, concentration statuses of CN in all the samples obtained from the investigated hand-dug wells were below detectable limits of 0.2mg/L (Table 1) as the comparative analysis of geochemical parameters from both sources are displayed in Figure 30. When the results of depicted heavy metal concentration values were compared with the guidelines set by World Health Organization (WHO, 2023), the outcome shows that the concentration values were all well within the stipulated permissible limits except for Mn, Cd, and Pb at ApeteWW₂, ApeteWW₃, and ApeteWW₁ respectively at 21m away from traverse 02, 35m away from traverse 03 and 20m away from traverse 01; all traverses at Apete cassava processing site indicating the occurrence of Mn, Cd and Pb at 0.26 mg/L, 0.004 mg/L alongside 0.02 mg/L respectively. The observed concentration of these heavy metals was above the WHO, 2023 allowable guidelines where the preponderance of Mn, Cd and Pb in the groundwater samples was attributable to the infiltration of CMEs into the subsurface groundwater system. The presence of Fe in other investigated sites that were void of CN most notably ApeteWW4 and ApeteWW5 is an indication of that the source of Fe may not be principally connected with CME; this could be possibly related to the local geology of the study area possessing iron content. The source of Fe content could be connected to the



Berkeley Journal of Entomology and Agronomy Studies

resultant leaching of Fe^{2+} from iron-bearing minerals such as Limonite, Goethite and Haematite that were residents within surface sediments which must have migrated its ways into the porous layers with unprecedented influence on the groundwater system of the study area (Etu-Efetor, 1981and Aweto et al., 2023). Migmatite-gneiss and other rock types in the study area have been found to contain principally of silica (S_iO_2), Alumina (Al_2O_3) and Iron-Oxide (Fe_2O_3) (Akinola and Obasi, 2020). High Iron content may also be attributed to acid solubilization subjected to prevailing acidic status of the soil (Amajor, 1985). It has also been discovered that groundwater is capable of attaining higher concentrations of heavy metals namely Pb, Fe, Cd, Mn and Cu as a result of the impact of acid rain leaching potential toxic metals through the surface soil to the underground groundwater system. When impermissible higher concentration of Iron is identified in the groundwater system, it may eventually result to the abandonment of boreholes tapping from such water (Ohwogbere-Asuma et al., 2020 and Aweto et al., 2023).

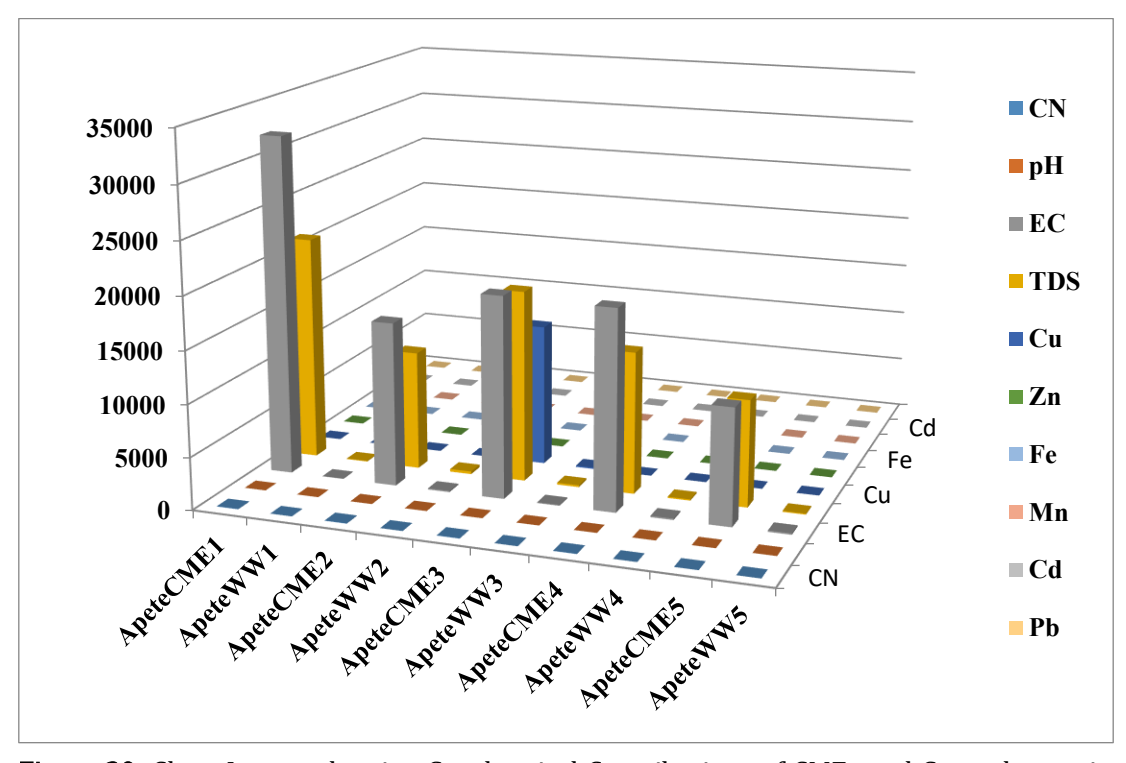


Figure 30: Chart Layout showing Geochemical Contributions of CMEs and Groundwater in Apete Cassava Processing Site

CONCLUSION

The 3D resistivity models and the VES in the research area showed resistivity values ranging from 3 to 200 Ω m and 27.4 Ω m to 65.5 Ω m respectively. Soil layers with resistivity values \leq

BERKELEY RESEARCH & PUBLICATIONS INTERNATIONAL Bayero University, Kano, PMB 3011, Kano State, Nigeria. +234 (0) 802 881 6063, berkeleypublications.com



E-ISSN 3027-2157 P-ISSN 3026-9482

Vol. 8, No. 1

Berkeley Journal of Entomology and Agronomy Studies

 $30\Omega m$ were identified as contaminated, which makes the soil layer conductive. The contaminated soil layer is believed to consist of sand, clay, and shale. The condition of the soil layers around the Apete Cassava processing site affects the horizontal and vertical distribution of leachate. It is suspected that the leachate may have seeped up to 40m (across the x-direction) up to 4m (across the z-direction) and up to 20m (across the y-direction) from the cassava processing site possibly by the migration of contaminant seepages to varying depths at the subsurface emanating from the cassava effluents at the surface. The distribution of leachate in the soil is estimated to occur from the surface to a depth of 40m, with accumulation in layers of clay-sand soil from 10m to 40m (across the x-direction). However, the distribution of the leachate tends to decrease with profile depth. The observed concentration of heavy metals was above the WHO, 2023 allowable guidelines where the preponderance of Mn, Cd and Pb in the groundwater samples was attributable to the infiltration of CMEs into the subsurface groundwater system. The investigation indicates that cassava processing has led to an increased concentration of liquid wastes principally comprising cyanides and cyanogenic glucosides within the soils of the investigated area. Furthermore, the outcomes suggest that the groundwater system of the study area is vulnerable to leachate infiltration most notably the shallow existing hand-dug wells in the area with depth ranging from 1.77m to 4.60m. This presents a bleak outlook for the future, foreseeing the gradual spread of existing aquifer contamination and the potential impact of cyanogenic glucoside compounds on the groundwater status of the study area.

REFERENCES

- Adebo B., Ilugbo S. O., Ozegin, K., Oyamenda, A. C., Oluwagbogo, Omotosho, O. A., Oduah, A. O. (2023). Impact of Landfills on Groundwater Quality Using Hydrochemical and Electrical Resistivity Methods at Apete/Awotan Area, Ibadan, Southwestern Nigeria. Earth Sciences Pakistan, 7(1): 01-10.
- Aizebeokhai, A. P (2010). 2D and 3D Geoelectrical Resistivity Imaging: Theory and Field Design. Scientific Research and Essays. Vol. 5(23). 3592–3605. http://www.academicournals.org/SRE
- Akinbiyi O. A, Oji A. S, Hansen-Ayoola A. O, Ugwoke J. L, Oladapo I. O, Isah A. (2018). Trace Element Geochemistry of Groundwater around Dump Site, a Case Study of Apete, South Western Nigeria *IJSER*. 809-813. http://www.ijser.org
- Akinola, 0.0 and Onasi, R.A (2020). Migmatite and Gneisses in the Basement Complex of Southwestern Nigeria: a Re-Appraisal of Their Structural, Mineralogical and Geochemical Diversity. IJRDO- Journal of Applied Science 2455-6653. 6(8): 1 –17.
- Alao, J.O. (2022). Impacts of Open Dumpsite Leachates on Soil and Groundwater Quality. Groundwater for Sustainable Development, 20 pp. 2-10, 2023. doi: 10.1016/j.gsd.2022.100877.
- Amanambu, A. C. (2015) Geogenic contamination: hydrogeochemical processes and relationships in shallow aquifers of Ibadan, South-West Nigeria. Bulletin of Geography. Physical Geography Series 9(1), 5-20. https://doi.org/10.1515/bgeo-2015-0011
- Aweto, K.E., Ohwoghere- Asuma, O., Ovwamuedo, G., and Atiti, P. (2023). Hydro-geochemical characterization and groundwater modeling of the subsurface around Ughelli West Engineered
- $Dump site in the Western \ Nigeria. \ Nigeria. \ Nigerian \ Journal \ of \ Technological \ Development. \ 20.\ 62-72.\ 10.4314/njtd.v20i2.1393.$
- Awoibi, J. and Ademakinwa G. O. (2018) Geophysical and Hydro-Chemical Investigations of Oke-Asunle Dumpsite in Ile-Ife, Southwestern Nigeria for Subsoil and Surface Water Pollution. Journal of Health and Pollution: 8 (20): 181209. https://doi.org/10.5696/2156-96148.20.181209.https://www.journalhealthpollution.org/doi/10.5696/2156-9614-614-





Vol. 8, No. 1

Berkeley Journal of Entomology and Agronomy Studies

- Azizah, S.N. (2016). Determination of Subsurface Leachate Distribution Using the Wenner-Schlumberger Configuration Geoelectrical Method in the Bandengan Village landfill Jepara Regency, Semarang State University,
- Broto, S., and Afifah, R.S. (2008). Geoelectric Data Processing with the Schlumberger Method, TEKNIK, 29(2), pp. 120-128, doi: 10.14710/teknik.v29i2.1939.
- Cheng, K., Simske S.J., Isaacson, D., Newell, J.C., Gasser, D.G (1990). Errors due to measuring voltage on current-carrying electrodes in electric current computed tomography. IEEE Trans. Med. Image. 37: 60–65.
- Cristina P., Cristina D., Alicia F. and Pamela B. (2012). Application of Geophysical Methods to Waste Disposal Studies, Municipal and Industrial Waste Disposal, Dr. Xiao-Ying Yu (Ed.), ISBN: 978-953-51-0501-5, https://www.intechopen.com/books/municipal-and-industrial-wastedisposal/application-of-geophysical-methods-to-waste-disposal-studies-
- Dahlin, L.T., Forsberg, K., Nilsson, A. and Flyhammer, P., (2006). Resistivity Imaging for Mapping of Groundwater Contamination at the Municipal Landfill La Chureca, Managua, Nicaragua. Near Surface 2006, 12th European Meeting of Environmental and Engineering Geophysics, 4-6 September; Helsinki, Finland
- Daruwati, I., (2019). Application of the Wenner Configuration Resistivity Geoelectrical Method to Determine Alleged Seepage of Garbage Pollutants Around the Final Disposal Site (Landfill) of Tanjung Belit Village, Rokan Hulu Regency, Edu Sains, 2(2), pp 77–80.
- Dey-Lewis, F.D., White, E.A., Johnson, C.D., Lane, J.W (2006). Continuous resistivity profiling to delineate submarine groundwater discharge- examples and limitations. Leading Edge 25:724-728.
- Egbinola, C. N. and Amanambu, A. C. (2014). Groundwater contamination in Ibadan, South-West Nigeria. SpringerPlus 3(1), 2-7.https://doi.org/10.1186/2193-1801-3-448.
- Etu-Efeotor, J. O. (1981). Preliminary hydrogeochemical investigation of subsurface waters in parts of the Niger Delta. Journal of Mining and Geology, 18(1):103 105.
- Fitrianti, A.N., (2018). Identification the Distribution of Seepage Of Toxical And Hazardous Materials using Geoelectrical Method (Case Study: Lakardowo Village, Jetis Sub-District, Mojokerto District), Maulana Malik Ibrahim State Islamic University.
- Feng, S.J., Zhao, Y., Zhang, X.L.and Bai, Z.B. (2020). Leachate Leakage Investigation, Assessment and Engineering Countermeasures for Tunneling Underneath a MSW Landfill, Engineering Geology, 265 (November 2019), 105447, doi: 10.1016/j.enggeo.2019.105447
- Ganiyu S. A., Badmus B. S., Oladunjoye M. A., Aizebeokhai A. P., Olurin O. T.(2015). Delineation of Leachate Plume Migration Using Electrical Resistivity Imaging on Lapite Dumpsite in Ibadan, Southwestern Nigeria. Geosciences 2015, 5(2): 70-80 DOI: 10.5923/j.geo.20150502.03
- Ganiyu, S. A., Badmus, B. S., Olurin, O. T. and Ojekunle, Z. O. (2018). Evaluation of Seasonal Variation of Water Quality Using Multivariate Statistical Analysis and Irrigation Parameter Indices in Ajakanga Area, Ibadan, Nigeria. Applied Water Science. Springer Berlin Heidelberg, 8(1): 35. doi: 10.1007/s13201-018-0677-y.
- Giang, N. V., Kochanek, K., Yu, N.T. & Duan, N. B. (2018). Landfill leachate assessment by hydrological and geophysical data: case study NamSon, Hanoi, Vietnam. Journal of Material Cycles and Waste Management, 203).1648-1662.doi:10.1007/810163-018-0732-7
- Helene, L.P.I., Moreira, C.A. and Bovi, R.C. (2020). Identification of Leachate Infiltration and Its Flow Pathway in Landfill by Means of Electrical Resistivity Tomography (ERT), Environmental Monitoring and Assessment, 192(4), 249. doi: 10.1007/s10661-020-8206-5.Heidelberg, 13-108.https://em.geosci.xyz/content/geophysical_surveys/mt/index.html https://en.m.wikipedia.org/wiki/Ibadan# :~:text=The%20city%20of%20Ibadan%20is,Centra%20part%20of%20the%20metropolis.
- Ishola S. A. (2019). Characterization of Groundwater Resource Potentials using Integrated Techniques in Selected Communities within Ewekoro Local Government Area South-West Nigeria. Department of Physics, FUNAAB Ph.D Thesis.
- Igbinosa, E. O. (2015). Effect of cassava mill effluent on biological activity of soil microbial community. Environmental Monitoring & Assessment, 187 (7): doi.10.1007/s10661-015-4651-y
- Igbinosa, E. O. and Igiehon, O. N. (2015). The impact of cassava effluent on the microbial and physicochemical characteristics on soil and structure. Jordan Journal of Biological Science, 8 (2): 107 112 in Southwestern Nigeria: Implications on Provenance and Evolution. Earth and Environmental Sciences. 97-118.
- Izah, S., Bassey, S. and Ohimain, E (2018). Impacts of Cassava Mill Effluents in Nigeria. Journal of Plant and Animal Ecology. 1. 14-42. 10.14302/issn.2637-6075.jpae-17-1890.



Berkeley Journal of Entomology and Agronomy Studies

- Karami, A.A., (2022). Modeling the leachate distribution pattern in the Ngipik landfill, Gresik Regency using the ogata-banks and Domenico-robbins analytical solutions, Sunan Ampel State Islamic University.
- Koefoed, O (1979). Geosounding principle, resistivity sounding measurements. Elsevier Scientific Publishing, Amsterdam.
- Lavrova, S. and Koumanova, B. (2010). Influence of Recirculation in a Lab-Scale Vertical Flow Constructed Wetland on the Treatment Efficiency of Landfill Leachate, Bioresource Technology, 101(6), pp 1756-1761, 2010. doi: 10.1016/j.biortech.2009.10.028
- Loke M. H. (2004). Tutorial: 2-D and 3-D Electrical Imaging Surveys. 2004 Revised Edition. www.geometrics.com P. 136
- Loke, M. H., (1999). Time-lapse resistivity imaging inversion. Proceeding of the 5th Environmental and Engineering Geophysical Society, Oct. 3-7, European Section, Belgium, pp. 123-125.1
- Meilasari, F., Sutrisno, H. & Purwoko, B., Analysis of Leachate Distribution around Batu Layang Landfill Area Based on Resistivity Value, Jurnal Teknologi Lingkungan, 24(1), pp. 10-20, 2023. doi: 10.55981/jtl.2023.247.
- Meju, M. (2000). Geo-electrical investigation of old/abandoned, covered landfill sites in urban areas: Model development with a genetic diagnosis approach, Journal Applied Geophysics, 44:115-150.
- Mendoza, M.B., Ngilangil, L.E. and Vilar, D.A. (2017). Groundwater & Leachate Quality Assessment in Balaoan Sanitary Landfill in La Union, Northern Philippines, Chemical Engineering Transactions, 56(2010), pp 247-252. doi: 10.3303/CET1756042.
- Mosuro, G.O, Bayewu, O.O Odugbesan, O. and Oloruntola, M . (2019). mapping subsurface leachate migration path using 3D electrical resistivity imaging at Farri dumpsite, ijebu ode, Southwestern Nigeria. 2. 95-102.
- Muhardi, M., Muliadi, M. and Zulfian, Z., (2020). 3D Model of Leachate Distribution in Soil Layers in the Batulayang Pontianak Landfill Area Based on Resistivity Values, JurnalllmiahFisika FMIPA Universitas Lambung Mangkurat, 17(2), 72, doi: 10.20527/flux.v17i2.7713.
- Naim, E.P. and Aprianto. A, (2016). Geotechnical Zonation Mapping in the City Pontianak Based on Data Consistency and Properties of Soil Using Geographical Information Systems, Jurnal Teknik Sipil, 16(2), pp. 1-16, https://jurnal.untan.ac.id/index.php/jtsuntan/article/view/19115.
- Nasir, K. A., Isaac, B. O. and Abraham, O. (2010). Detecting Municipal Solid Waste Leachate Plumes through Electrical Resistivity Survey and Physicochemical Analysis of Groundwater Samples. Journal of American Science, 6 (8): 18-35.
- NISP (2003). Nigerian Institute of Safety Professionals. Contractor Employee HSE Training Manual, Level 3, ECNEL Ltd, Port Harcourt, Nigeria.
- Nilasari, P.R., Khumaedi and Supriyadi, S (2012). Estimating the Distribution Pattern of Jatibarang Landfill Waste Using the Geoelectrical Method, Jurnal Pendidikan Fisika Indonesia, 7(1), pp. 1-5, 2011. doi: 10.1016/j.jenvrad..01.022.
- Nubatonis, H., Sutaji, H.I., Warsito, A. and Tanesib, J.L. (2021). Analysis of Leachate Distribution Patterns Around the Noenbila Landfill in South Central Timor District Using the Electromagnetic Conductivity Method, Jurnal Fisika Sains dan Aplikasinya, 6(1), pp. 2657-1900.
- Nwakaudu, M. S., Kanem, F. L. and Afube, G. A. (2012). Impact of cassava processing effluent on agricultural soil: A case study of maize growth. Journal of Emerging Trends in Engineering and Applied Science, 3 (5): 881 885
- Obueh H.O and Odesiri-Eruteyan E. (2016). A Study on the Effects of Cassava Processing Wastes on the Soil Environment of a Local Cassava Mill. Journal of Pollution Effects and Control. 4 (4): doi:10.4176/2375-4397.1000177
- Odjugo, P. (2010). The Impact Of Climate Change On Water Resources: Global And Nigerian Analysis. FUTY Journal of the Environment. 4. 10.4314/fje.v4i1.48005.
- $Ogata, A.\ (1990).\ The\ Theory\ of\ Dispersion\ in\ a\ granular\ medium.\ U.\ S.\ Geological\ Survey\ Professional\ Paper\ 411-1.$
- Ogbonna, C., Nwaugo, Victor, A. E and Chima, G. (2008). Impact of Cassava Mill Effluent (CME) on Soil Physicochemical and Microbial Community Structure and Functions. Nigerian Journal of Microbiology. 22. 1681 1688.
- Ogilvy, R., Meldrum, P., Chambers, J., & Williams, G. (2002). The use of 3D electrical resistivity tomography to characterize waste and leachate distribution within a closed landfill, Thriplow, UK. *Journal of Environmental & Engineering Geophysics*, 7(1), 11-18.
- Ogundana A. K, Aladesanmi A. O., Olutomilola O. O., Olowookere O (2018). Geophysical Investigation of Igbatoro Dumpsite, Southwest Nigeria, The International Journal Of Science & Technology, 6 (10): 68-75





Vol. 8, No. 1

Berkeley Journal of Entomology and Agronomy Studies

- Ohwoghere-Asuma, O., & Aweto, K.E. and Akpoborie, I. (2014). Investigations of groundwater quality and evolution in an estuary environment: A case study of burutu island, western Niger Delta, Nigeria. Journal of Environmental Hydrology. 22.
- Ohwoghere- Asuma, O., Chinyem, F., Aweto, K.E and Iserhien-Emekeme, R. (2020). The use of a very low-frequency electromagnetic survey in the mapping of groundwater conditions in Oporoza-gbamaratu area of the Niger Delta. Applied Water Science. 10. 10.1007/s13201-020-01244-w.
- Ojo, A.O., Olurin, O.T., Ganiyu, S.A., Badmus, B.S. and Idowu, O.A.(2022). Electrical Imaging Characterization of a Dumpsite on an Abandoned Quarry Site in Abeokuta, South West, Nigeria, Scientific African, 17, e01330,. doi: 10.1016/j.sciaf.2022.e01330.
- Oyedele, K.F. (2009). Total Dissolved Solids (TDS) Mapping in Groundwater using Geophysical method. New York Science Journal, 2(3): 10-15
- Okechi R, Ihejirika C, Chiegboka N and Ibe 1. (2012). Evaluation of the effects of cassava mill effluent on the microbial populations and physicochemical parameters at different soil depths. International Journal of Biosciences.;2(12):139-145
- Osakwe S. A. (2012). Effect of cassava processing mill effluent on physical and chemical properties of soils in Abraka and Environs, Delta State, Nigeria. Chemistry and Materials Research. 2(7): 27 39.
- Padmaja, G. (1995). Cyanide detoxification in cassava for food and feed uses. Critical Reviews in Food Science and Nutrition, 35(4): 299 339
- Parlinggoman, R.H. (2011). Study of Wastewater Distribution in the Northern Part of Bantar Gebang Landfill Using the Wenner-Schlumberger Resistivity Method, the University of Indonesia.
- Porsani, L.., Filho, W. M., Ellis, V. R., Shimlis, J.D. and Moura, H. P. (2004). The use of GRR & VES in delineating a contamination plume in a landfill site, A case study in SE Brazil. Journal of Applied Geophysics, 55:199-209.
- Pratama, R.I., Salim, N. and Setyaningtyas, R. (2020). Study of Predicting the Location of Leachate Accumulation Using the Wenner Configuration Resistivity Mapping Method (Case Study at Pakusari Landfill, Jember Regency).
- Pratiwi, D., Susanti, N. and Dewi, I. (2018). Application of Geolistric Method Wenner Mapping Configuration for Knowing Leachate River in Talang Gulo Jambi Landfill, Journal Online of Physics, 4(1).
- Priambodo, I.C., Purnomo, H. & Rukmana, N. (2011). Application of the Wenner-Schlumberger Configuration Geoelectrical Method in the Land Movement Survey in Bajawa, NTT, Pusat Vulkanologi dan Mitigasi Bencana Geologi Sari, 6, pp 1-10.
- Purwanta, W. (2007). Overview of Leachate Processing Technology in the Landfill, Jurnal Air Indonesia, 3(1), pp. 57-63, doi: 10.29122/jai.v3i1.2318. (Text in Indonesian)
- Putra, I K., Mahendra, M.S. & Ardana, I P.G. (2011). Identification of Seepage Direction and Location of Leachate Accumulation Using the Geoelectrical Resistivity Wenner-Schlumberger Configuration Method at Temesi Landfill, Gianyar Regency, Ecotrophic: Journal of Environmental Science, 7(1),pp 65-71, 2012.
- Qadri, U., Wahyuni, R. and Listiyawati, L. (2020). Application-based Waste Management Innovation with Environmental Insight in Pontianak City Eksos, 16(2), pp. 144–60. doi: 10.31573/eksos.v16i2.175.
- Rahaman, M. A. (1988). Recent Advances in the Study of the Basement Complex of Nigeria on Precambrian Geology Survey of Nigeria. Survey of Nigeria, 11-43.
- Riogilang, H. (2021). Seminar on Pollution Control and Spread of Leachate from Seepage Leachate Ponds in the Sumompo Manado landfill, 18(2), pp. 67-74.
- Sechman H., Moscicki W. J. and Dzieniewicz M., (2013). Pollution of the near-surface zone in the vicinity of gas wells. Geoderma, vol. 197-198, pp. 193-204, 2013.
- Sedana, D., As'ari, A. and Tanauma, A. (2015). The Mapping Of Groundwater Aquifers At The Ringroad Malendeng Village By Using Geoelectric Resistivity method, Jurnal Ilmiah Sains, 15(1), 33, doi: 10.35799/jis.15.1.2015.6778.
- Siller, H and Winter, J. (1998). Degradation of cyanide in agroindustrial or industrial wastewater in an acidification reactor or a single-step methane reactor by bacteria enriched from soil and peels of cassava. Applied Microbiology and Biotechnology. 50(3):384-389.
- Tampubolon, H., Zaenudin, A. and Antosia, R.M. (2020). Identification of Groundwater Pollution Due to Leachate Water Using Geoelectric Prisoners in TPS ITERA Jati Agung District, South Lampung Regency, 37th Eur. Ph Conf, 16(1).

BERKELEY RESEARCH & PUBLICATIONS INTERNATIONAL





06.30.2025

Pg.37

Vol. 8, No. 1

Berkeley Journal of Entomology and Agronomy Studies

- Telford, W.M., Geldart, L.P., Sherriff, R.E., Keys, D.A (1976). Applied Geophysics. Cambridge University Press, London, New York. pp. 860.
- Ulfani, B.D.A., Nurjannah, S. and Sugiyanto, D. (2019). Identification of Hydrogeological Effects on Leachate Spread in the East and West of the Java Gampong Landfill Using the Geoelectric Method, Aceh Phys Soc, 8(2), pp. 41-46. doi: 10.24815/jacps.v8i2.11245.
- World Health Organisation, WHO (2023). Guidelines for drinking water quality (3rd Eds. incorporating the 1st and 2nd Addenda) volume 1 recommendation .Geneva http://www.who.int/water sanitation health/dwq/gdwq3rev/en/. Accessed on 15th August, 2024.
- Yadi, K. (2017). Identification of Leachate Migration at Ngipik Landfill Gresik Using Very Low Frequency Electromagnetic (VLF-EM) Method, ITS, 2017.
- Yatim, E.M. and Mukhlis (2013). Effect of Waste Leachate on Residents' Well Water around Landfill Air Dingin, Jurnal Kesehatan Masyarakat, 7(2), pp. 54-59.